Helsinki University of Technology Radio Laboratory Publications
Teknillisen korkeakoulun Radiolaboratorion julkaisuja
Espoo, July 2003 REPORT 261

MODELING AND CHARACTERIZATION OF URBAN RADIO CHANNELS FOR MOBILE COMMUNICATIONS

Thesis for the degree of Doctor of Science in Technology

Hassan M. El-Sallabi

TEKNILLINEN KORKEAKOULU
TEKNISKA HÖGSKOLAN
HELSINKI UNIVERSITY OF TECHNOLOGY
TECHNISCHE UNIVERSITÄT HELSINKI
UNIVERSITE DE TECHNOLOGIE D'HELSINKI

Helsinki University of Technology Radio Laboratory Publications
Teknillisen korkeakoulun Radiolaboratorion julkaisuja
Espoo, July, 2003 REPORT S 261

MODELING AND CHARACTERIZATION OF URBAN RADIO CHANNELS FOR MOBILE COMMUNICATIONS

Hassan M. El-Sallabi

Dissertation for the degree of Doctor of Science in Technology to be presented with due permission for public examination and debate in Auditorium S4 at Helsinki University of Technology (Espoo, Finland) on the 7th of July 2003 at 12 o'clock noon.

Helsinki University of Technology
Department of Electrical and Communications Engineering
Radio Laboratory

Teknillinen korkeakoulu
Sähkö- ja tietoliikennetekniikan osasto
Radiolaboratorio

Distribution:
Helsinki University of Technology
Radio Laboratory
P.O.Box 3000
FIN-02015 HUT
Tel. +358-9-451 2252
Fax. +358-9-451 2152

ISBN 951-22-6627-X
ISSN 1456-3835

Otamedia Oy
Espoo 2003

Anything in the universe has a model. Researchers in all fields work for long time of their life to discover a very little.

The question is who made them?

My God, **ALLAH,** *the Omniscient, the Omnipotent, is the Creator of everything from what is smaller than atom's constituents to what is larger than Galaxies.*

It is my believe and faith.

Preface

First and foremost, I am thankful to my God ALLAH, the most gracious the most merciful for helping me to finish this dissertation. It is my believe in ALLAH that helped me persevere at times when it seemed impossible to go on.

The work constituting this thesis is the major part of my research results obtained mostly in the last three years in Radio Laboratory/SMARAD, Helsinki University of Technology (HUT). The work has been funded by HUT, the Graduate School in Electronics, Telecommunications, and Automation (GETA) and partly by the Academy of Finland through their center of excellence program. I am also grateful to Nokia Foundation, HPY Foundation, the Finish Society of Electronics Engineers, Center for Advanced Technology in Telecommunications (CATT), WSOY:n Kirjallisuussäätiö, and Ella and Georg Ehrnrooth Foundation for the financial support that I have received from them.

I am grateful to my supervisor professor Pertti Vainikainen for his support, valuable comments, stimulating discussions, and many ideas. I, absolutely always, thank him and professor Antti Räisänen for their encouragement and work to provide the financial support to make my research visit to the USA possible. I also owe a great debt of gratitude and thanks to professor Henry Bertoni, for providing me the opportunity to join his wireless group as a visiting scholar. I have learned a lot from him, not only science. I would like to thank him for introducing me to the diffraction problems and characterizing radio channels in the path domain. I also thank professor Pierre Degauque, University of Lille, France, and professor I.Tai Lu, Polytechnic University, USA, for reviewing the thesis as pre-examiners and for their valuable suggestions. I also thank professor Jun-ichi TAKADA, Tokyo Institute of Technology, Japan and Dr. Terhi Rautiainen, Nokia Research Center, Finland, for accepting the opponence job.

I would like to express my thanks to all people in the Radio Laboratory. I would mention the secretaries: Tuula Myllari and Stina Lindberg for taking care of all of practical issues with the university. Special thanks to Stina for her care and following up my matters in Finland during my research visit to the USA. Thanks to Lorenz Schmuckli for his immediate responses when computer problems have come up.

Living in another country is difficult socially but my Libyan friends made it easier and enjoyable. I would like to express my thanking to all Libyan friends and their families. I would like to mention specially Mohamed Elmusrati and his wife for their support and being close to me and my family during our crossing of the tough times. During my stay in USA, the Islamic society made life easy, I would mention the Egyptian community, who I really appreciate for their help and assistance and from whom I have learned real Islamic brotherhood. I would like to mention Dr. Hussein Elseisy and his wife whose deed follow their words and think of others' feelings. I am deeply indebted to their invaluable hospitality.

I am indebted to my mother and my late father for teaching me the importance of hard working and perseverance and instilling in me the confidence that I could succeed at whatever I could choose to do. I like to thank my brothers, sisters, father and mother in law for their continuous encouragement. I would like to thank my daughters, Thanaa and Fatema, for their smiles, their fun, and for always reminding me of the most important work that I will ever do is within my own family. Now, the time is to try to express my thanking feeling to my wife, Dr. Aisha, for what she has done to me during this work, for her patience, for her wishes that I succeed, for her unwavering support, for her subtle methods of encouragements, for her wisdom when I face problems, for the many sacrifices she has made. I tried to express in words but I did not find ones that may describe the feeling. I pray to ALLAH to reward her the best here and thereafter.

Hassan M. El-Sallabi Helsinki, June 12, 2003.

Abstract

Results of this thesis contribute in modeling and characterization of radio channels for future mobile communications. The results are presented mainly in three parts: a) modeling of propagation mechanisms, b) methodology of developing a propagation model, c) characterization of urban radio channel.

One of the main propagation physical phenomena that have an important role in diverting signals to non line of sight scenarios is the diffraction process. This thesis proposes diffraction coefficients that have better agreement with finite difference time domain solution and rigorous diffraction theory than the coefficient commonly used in propagation predictions for mobile communications. The importance of diffuse scattering has also been investigated and showed that this physical process may have a key role in urban propagation, with a particular impact on the delay spread and angular spread of the signal at the receiver.

This thesis proposes wideband propagation models for main and perpendicular streets of urban street grids. The propagation models are ray-based and are given in explicit mathematical expressions. Each ray is characterized in terms of its amplitude, delay, and angle of arrival, angle of departure for vertical and horizontal polarizations. Each of these characteristics is given in a closed mathematical form. Having wideband propagation model in explicit expression makes its implementation easy and computation fast. Secondary source modeling approach for perpendicular streets has also been introduced in this thesis.

The last part of the thesis deals with characterization of urban radio channels for extracting parameters that help in successful design of mobile communication systems. Knowledge of channel characteristics enables reaching optimum trade off between system performance and complexity. This thesis analyzes measurement results at 2 GHz to extract channel parameters in terms of Rake finger characteristics in order to get information that helps to optimize Rake receiver design for enhanced-IMT2000 systems. Finger life distance has also been investigated for both micro- and small cell scenarios. This part of the thesis also presents orthogonality factor of radio channel for W-CDMA downlink at different bandwidths. Characterization of dispersion metrics in delay and angular domains for microcellular channels is also presented at different base station antenna heights. A measure of (dis-) similarity between multipath components in terms of separation distance in delay and angular domains is introduced by the concept of distance function, which is a step toward in development of algorithm extraction and analysis multipath clustering.

In summary, the significant contributions of the thesis are in three parts. 1) Development of new diffraction coefficients and corrections of limitations of existing one for accurate propagation predictions for mobile communications. 2) Development of wideband propagation models for urban street grid. The novelty of the model is the development in explicit mathematical expressions. The developed models can be used to study propagation problem in microcellular urban street grids. 3) Presenting channel parameters that will help in the design of future mobile communication systems (enhanced-IMT2000), like number of active fingers, finger life distance, and orthogonality factors for different bandwidths. In addition, a technique based on multipath separation distance is proposed as a step toward in development of algorithms for extraction and analysis of multipath clusters.

TABLE OF CONTENTS

Thesis Publications

This thesis is based mainly on the following publications.

[P1] **H.M. El-Sallabi**, G. Liang, H.L. Bertoni, I. T. Rekanos, and P. Vainikainen, "Influence of diffraction coefficient and corner shape on ray prediction of power and delay spread in urban microcell," *IEEE Transaction on Antennas and Propagation, Special Issue on Wireless Communications*, vol. 50, no. 5, pp. 703–712, May 2002.

[P2] **H.M. El-Sallabi,** I.T. Rekanos and P. Vainikainen, "A new heuristic diffraction coefficient for dielectric wedges at normal incidence," *IEEE Antennas and Wireless Propagation Letters*, vol. 1, pp.165–168, 2002.

[P3] **H.M. El-Sallabi** and P. Vainikainen, "Improvement in a heuristic UTD diffraction coefficient," *IEE Electronics Letters,* Vol. 39, pp. 10-12, Jan. 2003.

[P4] V. Degli-Esposti, **H.M. El-Sallabi**, D. Guiducci, K. Kalliola, P. Azzi, L. Vuokko, J. Kivinen, P. Vainikainen, "Analysis and simulation of the diffuse scattering phenomenon in urban environment," in *Proc. XXVIIth General Assembly of the International Union of Radio Science* (URSI 2002), Paper no. 1734 in CD, Aug. 17-24, 2002.

[P5] **H.M. El-Sallabi** and P. Vainikainen "Physical modeling of line-of-sight wideband propagation in a city street for microcellular communications," *Journal of Electromagnetic Waves and Applications*, vol. 14, pp. 904–927, 2000.

[P6] **H.M. El-Sallabi** and P. Vainikainen "Radio Wave Propagation in Perpendicular Streets of Urban Street Grid for Microcellular Communications. Part I: Channel Modeling," *Progress In Electromagnetic Research* (*PIER*), vol. 40, pp. 229–254, 2003, an abstract version in *Journal of Electromagnetic Waves and Applications*, vol. 17, no. 8, pp. 1157-1158, 2003.

[P7] **H.M. El-Sallabi**, "Fast Path loss prediction by using virtual source technique for urban microcells," in *Proc. of the IEEE Veh. Technolog. Conference* VTC'2000-Spring, vol. 3, pp. 2183–2187, May 2000, Tokyo, Japan.

[P8] **H.M. El-Sallabi** and P. Vainikainen, "Influence of chip frequency on characterizing radio channels for Rake receiver fingers for CDMA systems in microcellular Environment," accepted for publications in *IEICE Transaction on Fundamentals of Electronics, Communications and Computer Sciences*, to appear in October 2003.

[P9] **H.M. El-Sallabi**, H. L. Bertoni, and P. Vainikainen, "Channel characterization for CDMA Rake receiver design for urban microcellular environment," in *Proc. of the IEEE Communication Conference*, ICC2002, vol. 2, pp. 911–915, April 2002, NYC, USA.

[P10] **H.M. El-Sallabi**, H. L. Bertoni, and P. Vainikainen, "Experimental Evaluation of Finger Life Distance for CDMA Systems," *IEEE Antennas and Wireless Propagation Letters*, vol. 1, pp. 50–52, 2002.

As a general guideline, the first author of each paper has the main responsibility of the manuscript. In papers [**P1**]-[**P6**], [**P8**]-[**P10**] and [**P1**], [**P9**], [**P10**], the work was supervised by professor Pertti Vainikainen and professor Henry Bertoni, respectively. G. Liang, in paper [**P1**], has developed the ray-tracing tool used in the paper. I.T. Rekanos in papers [**P1**], [**P2**] made the FDTD calculations. In paper [**P4**], the author of this thesis has extracted measurement parameters for comparison in the paper and participated in writing the manuscript.

1. Introduction

The last decade has seen an unprecedented growth in mobile communications. It has been reported that a new wireless subscriber signs up every 2.5 seconds [1]. The combination of the flexibility of radio communications with the quality of digital transmission has contributed to the success of these systems. No doubt that the future wireless systems must support significantly higher data rates than the current systems do. The third generation (3G) communication system known as International Mobile Telecommunication-2000 (IMT2000)/Universal Mobile Telecommunication System (UMTS) [2] will support a wide range of information services. Services may include voice, data, video and multimedia communications operating at bit rates up to 2 Mbps over the air interface [3]**.** With the expansion of Internet services, data transmission in fixed services is increasing very rapidly. Therefore, higher speed transmission capability, e.g., above 2 Mbps, is expected from future mobile communication systems. Such demands will increase in line with the extension of IMT-2000. Considering this perspective, studies of the fourth generation (4G) system have been started in various organizations. It is expected that the 4G systems will operate at bit rates at 100 Mb/s for mobility applications and 1 Gbps for WLAN applications [4].

The development and deployment of mobile communication systems requires careful characterizations of the propagation environment [5]-[11]. Radio propagation is the heart of mobile communications. Radio environment obstacles interact with electromagnetic waves in different ways, like reflection, transmission, diffraction, and scattering [12], [13]. As a consequence, the transmitted signal reaches the receiver through different propagation paths, which makes the radio propagation channel as a complex function of time, frequency, polarization, and space [10]-[21]. This results in multipath fading, delay and angular spreads and polarization cross coupling. Instead of suffering from impairments, radio interface techniques of future mobile systems will adapt to and even benefit from them, e.g., UMTS utilizes the Rake receiver by exploiting the delay dispersion characteristics [2]. Adaptive antennas at base station [22]-[25] reduce the interference by exploiting spatial domain and increase link capacity. Moreover, information theoretic research shows that multiple antennas at both ends of the communication channels may increase the capacity tremendously by exploiting the available independent parallel channels [26]-[27].

On the other hand, the knowledge of propagation phenomena is required for radio network planning to ensure the most cost-effective deployment of wireless system. In order to determine coverage areas, to estimate the interference between radio stations in the network and to reach optimal level for the base station deployment and configuration while meeting the expected service level requirements, accurate propagation prediction is needed. Ray techniques, although have some disadvantages as will be explained later, have been successfully used to model radio wave propagation in different radio propagation environments, such as indoor, microcellular and cellular environments [28]-[37]. The ray-based propagation models intend to reproduce the actual physical wave propagation process for a given environment. These models may allow performing wideband analysis including delay, angle of transmission, angle of arrival, and polarization of each propagation path. Characterizing these parameters give information that help in optimizing design of wireless systems and network planning including adaptive antennas [38].

1.1. Objectives of the Work

The objectives of this thesis work are mainly two folds. The first main objective is to develop wideband radio wave propagation model for microcellular communications in explicit mathematical expression. The explicit mathematical expression model (EMEM) makes implementation easy and computation fast. The EMEM approach divides the microcellular environment into three parts: a) propagation in the main street, where the base station (BS) is located, b) propagation in the perpendicular street, c)

propagation in the parallel street. Propagation in each street type is modeled separately. The propagation model is ray based. The model provides characteristics of each ray in terms of complex amplitude for both horizontal and vertical polarizations, delay, direction of arrival at the receiver, and direction of departure from transmitter. The model can be used in studying radio wave propagation problems in microcellular environment. The model is mainly based on diffraction and reflection propagation mechanisms. In order to accurately model propagation mechanisms, this thesis work proposes diffraction coefficients that give better agreement with the finite difference time domain (FDTD) [39] and the solution of the rigorous diffraction theory. Diffuse scattering propagation mechanism is also investigated for small cells. A proposal of modeling path loss in perpendicular street based on secondary source approach is also presented. The second objective is to characterize the urban radio channel by analyzing measurements results carried out in urban environments at 2 GHz. This characterization may give results that help in successful design of future mobile communication systems. Even though there are many propagation models and channel characterizations results in literature, the methodology of this thesis work is novel in having EMEM methodology, and characterizes urban radio channels in terms that are not commonly presented in the literature, e.g., finger life distance, channel orthogonality factor for W-CDMA downlink, and separation distance of multipath components.

1.2. Contents of the Thesis

The results in this thesis are presented mainly in three parts: 1) modeling of propagation mechanisms, 2) methodology of developing propagation model, 3) characterization of urban radio channels. The first part presents modeling of propagation mechanisms like reflection, transmission, diffraction and scattering. New heuristic diffraction coefficients and extension of an existing one are presented in [**P1**-**P3**]. Importance of diffuse scattering is investigated by comparison of measurement results with those of advanced 3D ray tracing tool including diffuse scattering [**P4**]. The second part of the thesis results presents propagation models for the main and perpendicular streets of urban street grid in microcellular environments. The EMEM for the main and perpendicular streets are presented in [**P5**] and [**P6**], respectively. The secondary source modeling approach is proposed in [**P7**]. The third part of the thesis is application oriented in terms of characterization of the radio channel. Model-based characterization of microcellular channel is presented Section 4.2 of this thesis summary. Characterization of the radio channel in terms of the influence of chip frequency on power contribution of fingers of Rake receivers for CDMA systems in microcellular environment is presented in [**P8**]. Rake finger characteristics for CDMA systems in small cells are presented in [**P9**]. Finger life distances for Rake receiver design for microcellular environment are presented in [**P10**]. Characterization of channel orthogonality factor for W-CDMA downlink is presented in Section 4.4 of this thesis summary. Section 4.5 presents characterization of radio channel dispersion metrics in delay and angular domains. Separation distances of multipath components are discussed in Section 4.6.

2. Modeling of Propagation Mechanisms

The radio wave propagation through some physical environment is affected by various propagation mechanisms, which affect the quality of the received signal. The mechanisms behind electromagnetic wave propagation are diverse but can generally be attributed to reflection, transmission, diffraction and scattering. In urban environment, these effects can include diffraction caused by obstacles along the propagation path, such as buildings in urban environment. Radio wave signals are also specularily and/or diffusely reflected off obstacles or the ground and cause multi-path effects. The radio signal can be significantly attenuated by various environmental factors such as propagation through vegetation. When line-of-sight (LOS) propagation is not present, these environmental propagation mechanisms have the dominant effect on the received signal through dispersive effects, fading, and signal

attenuation. Ray-based modeling techniques enable accurate determination of propagation paths in LOS and non-line of sight (NLOS). These techniques are based on above-mentioned physical processes. Thus, accurate modeling of these propagation mechanisms is of paramount importance for accurate prediction of radio wave propagation by ray-based models.

2.1. Free Space Propagation

A free-space model characterizes the contribution to the signal at the receiving antenna due to the direct ray incident upon the receiving antenna. The power received by receiver antenna, which is separated from a radiating transmitter antenna by a distance *r,* assuming a free space path between the antennas, is given by the Friis free-space formula [40]-[41],

$$P_r = \frac{P_t G_t G_r}{L}\left(\frac{\lambda}{4\pi r}\right)^2 \tag{2.1}$$

and channel transfer function of the direct ray path is defined as

$$H(f,r) = \frac{\lambda}{4\pi r} e^{-jkr} \tag{2.2}$$

where P_t is the transmitted power, G_t and G_r are the transmitter and receiver antennas gain, respectively, L is system loss (L>1).

2.2. Specular Reflection Process

In general, reflection can occur from surfaces of any object, and these objects need not be planar. However, in wireless communication environments, the most commonly encountered reflecting obstacles such as buildings, are planar in form. For different heights of transmitter and receiver, rays incident on and reflected off a building surface travel obliquely to the face in both the vertical and horizontal planes, even for a vertically and horizontally polarized transmitter, the fields incident on the building face is not pure parallel or perpendicular to the surface, so that polarization coupling will take place. For transmitted field with vertically or horizontally polarized field components are transformed and become the parallel "||" and the perpendicular "⊥" polarized field components [43], [44], referring to a plane determined by the wall normal direction and incident, or reflection ray direction. An angle φ_i in a plane perpendicular to the incident ray offsets the two sets of field components. Inversely, prior to the reception by the receiver the last transformation takes place from "||" and "⊥" to horizontally and vertically polarized field components. In this thesis work in [**P5**], a reflection coefficient that includes the polarization transformation in the reflection coefficient for accurate calculation of wall reflection loss is proposed. In order to check the effect of the height difference of transmitter and receiver antennas on a reflection loss of one reflection order, the reflection coefficient is given by

$$\Gamma_{iVV,iHH} = \left(R_{\perp,\|}\ \cos^2\varphi_i - R_{\|,\perp}\sin^2\varphi_i\right) \tag{2.3}$$

$$\cos\varphi_i = \frac{xr_i}{\sqrt{x^2+\Delta h^2}\sqrt{x^2+\left(w-y_1+y_o\right)^2}} \tag{2.4}$$

where r_i the path length between the transmitter and the receiver, Δh is the height difference of the antennas, y_1 and y_0 are the distances between transmitter and receiver to building surface, and x is the distance difference between the two terminals, (see Figure 1 in [**P5**]). At large distances x, where $\Delta h \approx 0$, Eqn. (2.4) reduces to $\Gamma_{iVV,iHH} \approx R_{\perp,\parallel}$. Now the polarization coupling due to reflection is negligible and we may simply use the parallel or perpendicular Fresnel reflection coefficient ($R_{||,\perp}$) for calculation of reflection loss. The expression for multiple reflections of a ray bouncing between two walls is proposed in [**P5**]. Figure 2.1 shows magnitudes of $\Gamma_{iVV,iHH}$ and $R_{\parallel,\perp}$ in order to investigate the effect of difference of antenna height at different distances. The magnitude of this coefficient is significantly different from that of Fresnel reflection coefficient when the distance between transmitter and receiver is small. This is the case of indoor communications and may be more accurate in calculating reflected field of ultra wideband signals in room scenarios.

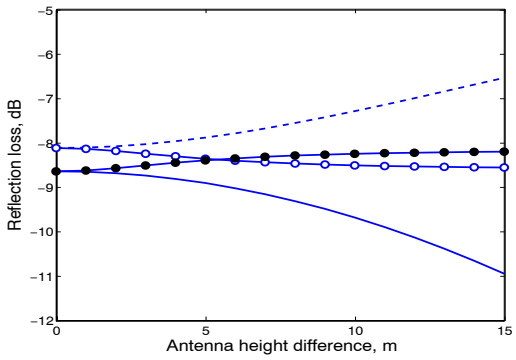

(a)

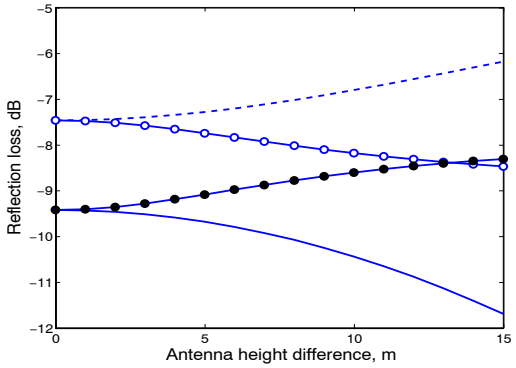

(b)

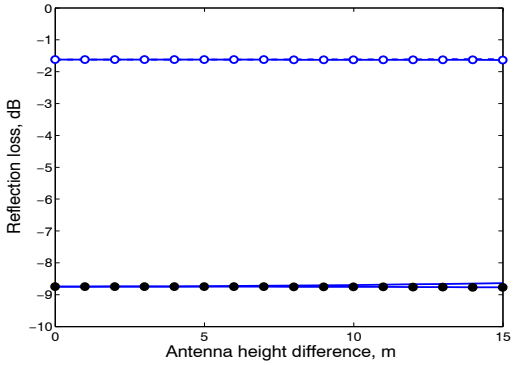

(c)

Figure 2.1. Impact of antenna height on reflection loss with w=20 m, y_0 = 2 m, y_1 = 3m, ε_r = 5; σ = 0.005 S/m. (a) x = 5. (b) x = 10. (c) x = 100.

$R_{\perp}$, $R_{//}$, Γ_{vv}, Γ_{hh}.

2.3. Transmission and Refraction Process

Transmission occurs when the radio wave encounters an obstacle that is to some extent transparent for the radio waves. This mechanism allows the reception of radio signals inside buildings in cases where the actual transmitter locations are either outdoors or indoors. Transmitted rays can be evaluated through the use of geometrical optics. Signals propagation through buildings are usually small in outdoor propagation. Refraction behind right angle wedges, i.e., building corners, requires permittivity of ε_r<2 [42]. Such corners rarely exist in microcellular environment.

2.4. Diffraction Process

Diffraction occurs when the radio path between the transmitter and the receiver is obstructed by a surface that has sharp irregularities (edges). In mobile communication environments, the primary diffracting obstacles, which perturb the propagating fields are buildings. The majority of contemporary structures are essentially rectangular in prisms that comprise a number of faces intersecting at straight edges of finite lengths. Thus, corners can be considered as wedges and diffraction theory can be applied. Diffraction formulas are well established

for perfectly conducting (PC) infinite wedges [44], [45], for absorbing wedges (AW) [46], and for impedance surface wedges [47]-[51]. The PC diffraction coefficients are accurate when dealing with diffraction phenomena arising from metallic objects. However, many important applications, such as in mobile communications, involve large dielectric structures with losses. In this case, the assumption of PC boundary conditions results in a lack of accuracy in predicting the actual electromagnetic field. On the other hand, the impedance-surface diffraction formulas are rather cumbersome to use for propagation prediction in mobile communications. Thus, the difficulty of using the rigorous solutions for propagation prediction forces simplifications to be made. Some existing diffraction coefficients [52]-[56] modify the PC-UTD diffraction coefficient in order to make it applicable to dielectric wedges with losses. Types of building corners can be represented as hollow or solid wedges. The field beyond the hollow wedges is higher than that of the solid wedges. This makes a need of diffraction coefficient for each type. The above-mentioned diffraction coefficients are for solid wedges. The hollow wedge diffraction coefficient is still one of the open questions in diffraction modeling. This thesis work proposes two new heuristic diffraction coefficients and improvement to existing one. The first proposed diffraction coefficient is based absorbing wedge solution (Sec. 2.4.1, [**P1**]). The second proposed diffraction coefficient is based on PC-UTD, (Sec. 2.4.2, [**P2**]). In addition, corrections to existing diffraction coefficient developed by Holm [56], (Sec. 2.4.3, [**P3**]). The proposed diffraction coefficients are valid for normal incidence with respect to the edge of the wedge.

2.4.1. AW-based diffraction coefficient [**P1**]

As mention earlier, the diffracted field in hollow wedges is higher in the deep shadow region, we can propose diffraction coefficient for hollow wedges by utilizing the results from perfectly absorbing wedge (AW) and extend them to applicable for no-perfect AW. In [**P1**] a new heuristic diffraction coefficient based on Felsen's diffraction coefficient for perfectly absorbing wedge [46] is proposed. The perfectly absorbing wedge is defined by the condition that the incident rays striking the wedge surface are completely absorbed at the wedge faces, so no reflected rays exist. The ray striking the edge, however, is scattered in all directions and gives rise to the spectrum of diffracted rays. Felsen's coefficient can be written as

$$D(\phi,\phi') = -\frac{1}{\sqrt{2\pi k}}\left(\frac{1}{\pi-\left|\phi-\phi'\right|}F(kLa^{-}(\phi-\phi'))+\frac{1}{\pi+\left|\phi-\phi'\right|}F(kLa^{+}(\phi-\phi'))\right) \tag{2.5}$$

which is extended in [**P1**] to include the reflection shadow boundary for a non-perfectly absorbing wedge. The extension is given as

$$D(\phi,\phi') = -\frac{1}{\sqrt{2\pi k}}\left(\begin{array}{l}\dfrac{1}{\pi-\left|\phi-\phi'\right|}F(kLa^{-}(\phi-\phi'))+\dfrac{1}{\pi+\left|\phi-\phi'\right|}F(kLa^{+}(\phi-\phi')) \\ +\Gamma_0\dfrac{1}{\pi-(\phi+\phi')}F(kLa^{-}(\phi+\phi'))+\Gamma_n\dfrac{1}{(\phi+\phi')-(2n\pi-\pi)}F(kLa^{+}(\phi+\phi'))\end{array}\right) \tag{2.6}$$

whichever is greater in magnitude. The angle ϕ' and ϕ are the incident and diffracted ray angles with respect to the illuminated face of the wedge and n is related to the internal angle of the wedge ψ by the relation $\psi=(2-n)\pi$, (see Figure 2.2), $\Gamma_{o,n}$ is the Fresnel reflection coefficient for parallel and perpendicular polarizations. Diffraction coefficient in Equation (2.5) includes only the incidence shadow boundary. The two additional terms in Equation (2.6) are added heuristically in [**P1**] to represent the reflection shadow boundary, which does not exist in Felsen's diffraction coefficient for an

absorbing wedge [46]. The functions $F\left(kLa^{\pm}\left(\phi \pm \phi'\right)\right)$ are related to the complementary error function, and are defined in [44],[45],[52]. These functions are responsible for making the field continuous across the shadow boundaries.

2.4.2. PC-UTD-based diffraction coefficients [**P2**]

This diffraction coefficient is for solid wedges (losses are high). The PC-UTD diffraction coefficient involves the sum of four terms. In order to treat imperfectly conducting (i.e., lossy dielectric) wedges, the authors of [52],[56] multiplied each of these terms by additional factors to make the diffraction coefficients applicable to lossy dielectric wedges. In this thesis work, a general form of the PC-UTD-based diffraction coefficient that makes existing PC-UTD-based solutions as special cases of it is proposed in [**P2**]. The general form can be expressed as:

$$
\begin{aligned}
D = & \frac{\exp\left(-j\pi/4\right)}{2n\sqrt{2\pi k}} \\
& \cdot\left\{\Gamma_1 \cot\left[\frac{\pi+\left(\phi-\phi'\right)}{2n}\right]F\left[kLa^{+}\left(\phi-\phi'\right)\right]+\Gamma_2 \cot\left[\frac{\pi-\left(\phi-\phi'\right)}{2n}\right]F\left[kLa^{-}\left(\phi-\phi'\right)\right]\right. \\
& \left.+\Gamma_3 \cot\left[\frac{\pi-\left(\phi+\phi'\right)}{2n}\right]F\left[kLa^{-}\left(\phi+\phi'\right)\right]+\Gamma_4 \cot\left[\frac{\pi+\left(\phi+\phi'\right)}{2n}\right]F\left[kLa^{+}\left(\phi+\phi'\right)\right]\right\}
\end{aligned}
\tag{2.7}
$$

where $F(\bullet)$ is the transition function, and n is related to wedge angle (Fig. 2.2). Detailed descriptions of the variables that appear in (2.7) are given in [44],[45]. Different definitions of multiplication factors Γ_i (i = 1,…,4) of each term in (2.7) result in different diffraction coefficients that exist in literature. For $\Gamma_{1,2,3,4}=1$, and $\Gamma_{1,2}=1$, $\Gamma_{3,4}=-1$, we obtain the PC-UTD diffraction coefficient for perpendicular and parallel polarizations [44],[45], respectively. Discussion of other diffraction coefficients as special cases of (2.7) is presented in [**P2**]. In this thesis work in [**P2**], a new definitions of the multiplication factors Γ_i for i = 1,..,4 is introduced by utilizing a coefficient that was inferred from suitable formulation of the Maliuzhinets' solution [48],[51],[57], which is given by

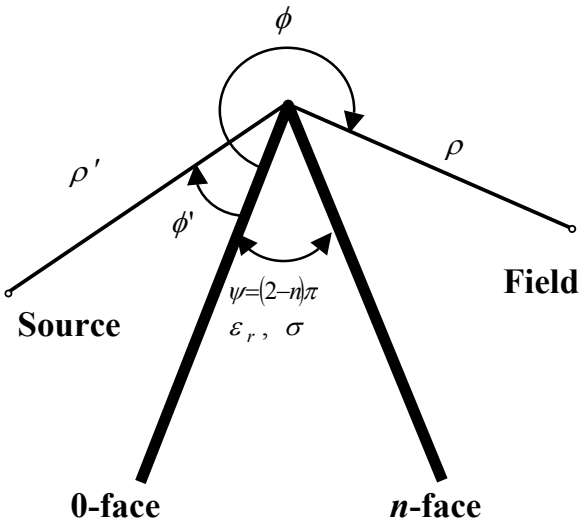

Figure 2.2. Geometry of diffraction by a non-perfectly conducting wedge.

$$
\Re^{\parallel,\perp}=\frac{\left(1,\varepsilon_r\right)\tau-\sqrt{\varepsilon_r-1+\tau^2}}{\left(1,\varepsilon_r\right)\tau+\sqrt{\varepsilon_r-1+\tau^2}} \tag{2.8}
$$

$$
\tau = 2\sin\left(\frac{\phi}{2}\right)\sin\left(\frac{\phi'}{2}\right). \tag{2.9}
$$

In [**P2**], the multiplication factors Γ_i in (2.7) are defined as $\Gamma_{1,2}=1$, and $\Gamma_{3,4}=\Re^{\parallel,\perp}$ where $\Re^{\parallel,\perp}$ is given in (2.8) for parallel or perpendicular polarizations. The diffraction coefficient has to work for

both scenarios when the source either faces one side or two sides of the wedge. This has influence on the definitions of ϕ and ϕ' in (2.9). If the source illuminates both sides of the wedge (*i.e.*, $\phi' > ((n-1)\pi)$ and $n \geq 1.5$, $\phi > \pi$, the angles ϕ and ϕ' in (7) change to $n\pi - \phi$ and $n\pi - \phi'$, respectively, otherwise no change in the earlier definition (Fig. 1). If $\phi > ((2n-1)\pi - \phi') \cup \phi > \pi$ and $n < 1.5$ and, angles ϕ and ϕ' in (3) change to $n\pi - \phi$ and $n\pi - \phi'$, respectively, Otherwise no change takes place. The originality of this thesis work is in the improvement in the accuracy of calculation of the diffraction coefficient for lossy dielectric wedges with respect to solutions in [52], [56] when they are compared to the rigorous solution and FDTD simulations. The improvement is achieved by introducing the modified reflection coefficient (2.8), with the definition of ϕ and ϕ' as stated earlier, instead of the commonly used Fresnel reflection coefficient as a multiplication factor for the characteristic terms of the PC-UTD solution. Though the definition of ϕ and ϕ' is somewhat cumbersome, it anyway makes the computation much faster than the calculation of Maliuzhinets functions.

2.4.3. Improvement in diffraction coefficient for non-perfectly conducting wedges **[P3]**

Holm has proposed in [56] a heuristic UTD diffraction coefficient for non-perfectly conducting, lossy dielectric, wedges as an extension to the heuristic one given by Luebbers [52]. This is also for solid wedges. The reflection coefficients in Holm's formulations, R_o and R_n are calculated with reflection angles θ_o, θ_n, corresponding to the angular location of the source with the observation point relative to the normal of the incidence and diffraction faces (i.e., *o* and *n*-faces), respectively. In this thesis work in [**P3**], it is shown that the accuracy of the calculation of the diffracted field can be significantly increased by redefining the angles at which the Fresnel coefficients are computed. If the source illuminates the *o*-face or the *n*-face of the wedge, the reflection angles with respect to the normal on the faces of the wedge are defined as $\theta_o = \pi/2 - \phi'$ and $\theta_o = \pi/2 - (n\pi - \phi')$, respectively, for calculation of R_o. The definitions of θ_n needed for calculation of R_n are presented in Table 2.1. The first and the second lines in Table 2.1 depend on the observation angle if it is before or beyond the reflection shadow boundary, respectively, which is determined by $\phi + \phi' = \pi$ or $\phi + \phi' = (2n-1)\pi$ when the source illuminates the *o*-face or *n*-face, respectively.

Table 2.1. Definition of the reflection angles, relative to normal on a face, used in calculation of Fresenl reflection coefficient involved in computation of diffraction coefficient.

Illuminating *o*-face	Illuminating *n*-face	Luebbers & Holm Illuminate (*o*-face, *n*-face)		New
Region	Region	θ_o	θ_n	θ_n
$\phi < (\pi - \phi')$	$\phi < \pi \cap \phi < \lvert(2n-1)\pi - \phi'\rvert$	$\lvert\pi/2 - (\phi', \phi)\rvert$	$\lvert(\phi, \phi') + (0.5 - n)\pi\rvert$	$\lvert\pi/2 - \phi\rvert$
$\phi < \pi \cap \phi > (\pi - \phi')$	$\phi < \pi \cap \phi > \lvert(2n-1)\pi - \phi'\rvert$	$\lvert\pi/2 - (\phi', \phi)\rvert$	$\lvert(\phi, \phi') + (0.5 - n)\pi\rvert$	$\lvert\phi + (n - 2.5)\pi\rvert$
$\phi > \pi$	$\phi > \pi$	$\lvert\pi/2 - (\phi', \phi)\rvert$	$\lvert(\phi, \phi') + (0.5 - n)\pi\rvert$	$\pi/2 - (n\pi - \phi)$

Illumination of one side, i.e., $\phi' < (n-1)\pi$, or two sides, i.e., $\phi' > (n-1)\pi$ of a wedge, are quite common scenarios as building corners in microcellular environment. In propagation scenarios like perpendicular street, the source illuminates one and two faces of the perpendicular street corners. The diffracted field due to these different scenarios has to be accurate. The improved version of Holm's diffraction coefficient works quite well and very close to the rigorous solution for the case of

illumination of one face and gives poor results when the source illuminates two sides of the building corner. However, the solution presented in Section 2.4.2. gives close agreement to the rigorous solution, in mean square error sense, when the source illuminates the two faces of the wedge.

2.5. Scattering Process [P4]

Rough surface causes scattering into the non-specular directions and reduction of energy in the specular direction. The influence of rough surface depends on the degree of roughness. The longer the wavelength and the smaller the grazing angle, the weaker is the effect of surface irregularities. The importance of roughness has been determined by measurements [58]. In some scenarios, the roughness is so significant that no coherent part is re-transmitted toward the receiver. If the diffuse reflection is isotropic, then the intensity in any direction varies as the cosine to the angle between that direction and the normal to the surface. The influence of the surface can be described by a simple cosine relation called Lambert's cosine law. In urban propagation, diffuse scattering can be considered as originating from building wall surfaces. In order to model diffuse scattering in an urban environment, a sort of effectiveness is associated with each building wall. This takes into account the real surface roughness, wall discontinuities, small object effects, etc. [59]. The scattering contribution of each wall is computed from the distance of each wall and orientation with respect to the transmitter and the receiver using a formula which depends on a few scattering parameters. Diffuse scattering has been modeled according to the *effective roughness approach* expressed with an integral approach for close by objects described in [59], or with a simplified approach for far away objects, which is important for wideband prediction [60]. The latter is expressed as

$$E_S^2 = K_0^2 S^2 \frac{Area \cdot \cos\theta_i \cos\theta_s}{\pi} \frac{1}{r_i^2 r_s^2}. \qquad (2.10)$$

The variables in (2.10) are defined in [60]. In [**P4**], measurement data are analyzed to extract the following parameters: path loss, delay spread and direction spread. The experimental results are compared to simulations performed with those of an advanced 3D ray-tracing model, which takes diffuse scattering into account in the form presented in (2.10). The included mechanisms in the tested version of the ray tracing model are over-rooftop propagation and diffuse scattering. The comparison shows acceptable agreement between ray tracing including diffuse scattering and over roof top

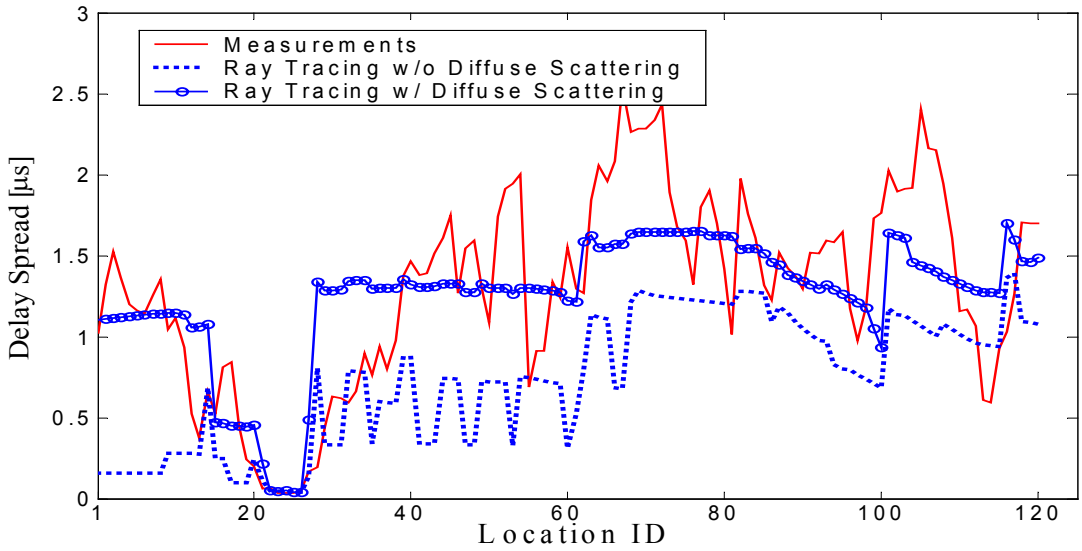

Figure 2.3. Comparison of measured delay spread with that from ray tracing with and without diffuse scattering.

propagation and measurements. In order to investigate what role the diffuse scattering mechanism plays over other mechanisms, Figure 2.3 shows a comparison of conventional ray tracing (i.e., reflection and diffraction mechanisms are included without diffuse scattering) and a version where scattering is included. It can be seen clearly that the inclusion of diffuse scattering has improved the prediction of rms delay spread when compared to conventional full 3D ray tracing. From this comparison, we are able to understand the importance of the role of the diffuse scattering. This work is still under investigation in co-operation with the propagation research group at University of Bologna, who developed the idea described in (2.10).

3. Modeling of Radio Wave Propagation in Microcells

3.1. Introduction

Modeling of radio wave propagation is very important for prediction tools for RF design in dense urban areas. Microcell is defined as a cell located in a dense urban area, providing less than 1 km coverage on generally flat terrain, and embedded within a cluster of buildings. Generally, the propagation models can be classified either empirical or deterministic (i.e., the most common in literature is the site-specific modeling approach), or a combination of these two. There are many empirical and deterministic models for propagation prediction [61]-[86]. The empirical models are derived from measurement results. The theoretical, *i.e.,* deterministic models, are based on the fundamental principles of radio wave propagation physics. Due to that, they can be applied to different environments without affecting the accuracy. This approach is able to determine the dominant paths. It takes into account more details of the environment by approximating certain elements of the environment (buildings, terrain, etc) by geometrical shapes with certain electrical properties. The advantages of empirical approaches are their relative simplicity of implementation and speed of computation when compared to deterministic approaches. They can also incorporate physical mechanisms, which are not obviously identifiable or calculable by a deterministic approach, e.g., the attenuation effect of trees, where most of models are empirical. The main disadvantage of empirical models is that they provide little insight into the propagation phenomena. Therefore, it is hard to track and analyze the source of errors in comparison with measurements. On the other hand, the accuracy of these models depends not only on the accuracy of the measurements, but also on the similarities between the environment to be analyzed and the environment where the measurements are carried out. The strength of site-specific (i.e., deterministic) approaches is the understanding they provide on the basic physical processes behind radio wave propagation. It is easier to track and analyze sources of errors with measurements. The main disadvantages of deterministic approaches are: 1) they may be difficult to implement, 2) they are slower to run, 3) they require a detailed description of the environment, which is sometimes expensive or even impossible to obtain.

In this thesis work, the adopted modeling approach is the deterministic method. The developed modeling approach proposes a methodology that overcomes the first, second and partly the third of the above-mentioned limitations by giving the propagation model in an explicit mathematical expression. The advantages of the EMEM are that it is easy to implement and easy to use for studying propagation problems in addition to fast computation since it is given in a closed form. The model requires the environment database in terms of positions of street corners. There are mainly two ray tracing approaches: image-based and ray launching. Image-based approach finds all rays for each receiving point individually and guarantees the consideration of each wall. This approach consists of two main steps: the creation of the visibility tree and the backtracking procedure. This individual computation is more time-consuming than the ray launching approach, where a large number of rays with a constant angular separation between neighboring rays are launched from a transmitter and intersection tests are performed for each ray on every scatter to determine the scattering points. After locating each scattering point, the reception test based on the reception sphere concept is performed. This method is

applicable to complex environments, but enormous computation time and memory are required due to large number of rays and tests. Furthermore, the accuracy of the predicted result is sensitive to the separation angle, which in fact decreases the resolution with growing distance from the transmitter. As a result the transmitter may not see different building corners if they are close to each other. The proposed approach is different from these approaches in a sense that there is no searching for the coupling radio paths between the transmitter and the receiver since ray characteristics are given in a closed mathematical form, where no generation of visibility tree and backtracking procedure takes place, which usually takes long time. Also there are no reception tests in the proposed approach. As the proposed solution is image based, it has higher resolution than the ray launching approach. The proposed approach determines sets of angles of rays that do not couple transmitter and receiver. These sets are determined by knowledge of the positions of transmitter and receiver as well as building corners. Having closed form of characteristics of each ray makes calculation fast to check if a ray belongs to these sets or not. This thesis work also proposes path loss modeling approach based on the secondary source principle.

3.2. Modeling of Radio Wave Propagation in City Street Grid

The adopted modeling methodology in developing the propagation model classifies the city street grid into three main parts. The different along streets radio wave propagation types are shown in Figure 3.1: a) the main city street (i.e., solid line) radio wave propagation scenario, *i.e.,* the MS is in the LOS with the BS, b) the perpendicular street (i.e., dased lines) radio wave propagation scenario, *i.e.,* the MS is the perpendicular street with respect to the street where the BS is located, c) the parallel city street (i.e., dotted lines) radio wave propagation scenario. In this thesis, only models for the first and second propagation scenarios are presented. The third propagation scenario can be modeled by combining perpendicular street propagation model with the secondary source modeling approach (Sec. 3.3).

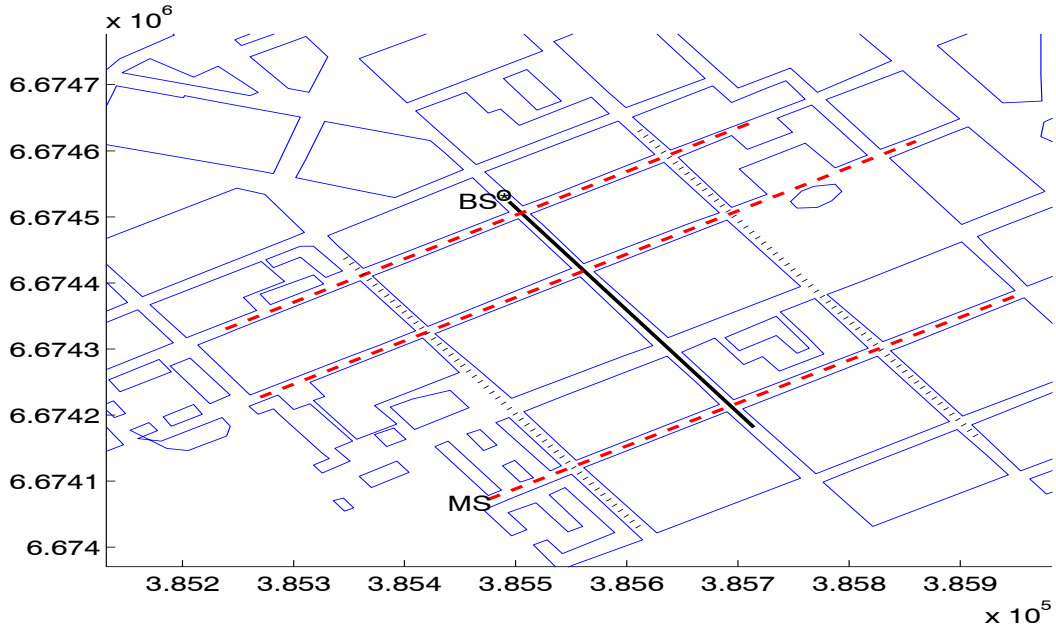

Figure 3.1. Sample of a microcellular environment.

Each model of different propagation scenario provides ray propagation information at both the BS and MS. The height of antennas is assumed to be below the rooftops of the surrounding buildings, so rays diffracted over the building rooftops are neglected. It is assumed that the streets are flat, straight, and

lined with tall buildings whose walls are assumed to be smooth flat surfaces with average relative permittivity. The developed model determines the coupling radio paths based on set membership criteria. The proposed model is not only capable to provide macroscopic quantities like mean field values and rms delay spread, but also the full wideband channel information, *i.e.,* space dependent complex channel responses with a high time dispersion resolution. The model is based on deriving the channel transfer function $H(f,r)$ of a spatial variant multi-ray model, where f is the frequency and r is the path length.

3.2.1. Modeling of radio wave propagation in the main city street **[P5]**

In this thesis work, a propagation model is based on deriving the channel transfer function. Image theory and horizontal plane angle criterion are utilized to find possible coupling radio paths. The channel transfer function of all considered rays that strike walls up to m times is given by

$$H(f,r) = \sum_{i\equiv(S,m,g)} f_B(\theta_i,\phi_i) f_M(\Theta_i,\Phi_i) H_i \delta(\Pi(S)) - \Pi(m)) \tag{3.1}$$

$$H_i = \Gamma^i_{VV,HH} \lambda e^{-jkr_i} / (4\pi r_i), \tag{3.2}$$

$$\Gamma^i_{VV,HH} = (\Re^i_{V,H})^g \left((R^i_{H,V})^m \cos^2\varphi_i + (-1)^m (R^i_{V,H})^m \sin^2\varphi_i \right), \tag{3.3}$$

$$\Pi(\chi) = \begin{cases} 0, & \chi = 0 \\ 1, & \chi > 0 \end{cases}. \tag{3.4}$$

where H_i is the transfer function of ray i, which is represented by three integers (S, m, g), m is the reflection order, S = 1, (2) for BS images with first reflection on the wall $-y_1$ and (w_1-y_1), respectively, g = 0,1 is for ground reflection, λ is the wavelength, k is the wave number, $\delta(\bullet)$ is the delta function, $\Gamma^i_{VV,HH}$ is the co-polarized reflection coefficient of ray i for vertical and horizontal polarization, respectively, $\Re^i_{V,H}$ and $R^i_{H,V}$ are the well-known Fresnel reflection coefficients for the ground and wall reflections, respectively, with transmission in vertical and horizontal polarization of ray i. When a crossing street exists between the BS and MS, the wall-reflected coupling rays are determined by the horizontal plane angles of ray i as

$$\alpha_i \notin \bigcup_{p=1}^{j} \bigcup_{q=1}^{m} \left\{ \alpha : \alpha_{pWG2} < \alpha < \alpha_{pWG1} \right\} \tag{3.5}$$

$$\alpha_{pWG\xi} = \arctan\left(\frac{(q + (S-2))w - (-1)^S y_1}{x_{pWG\xi}} \right) \tag{3.6}$$

$$G = S - (-1)^S \Xi(q+1) \tag{3.7}$$

$$\Xi(\chi) = \begin{cases} 0, & \forall\, \chi \text{ even} \\ 1, & \forall\, \chi \text{ odd} \end{cases}, \tag{3.8}$$

where p = 1,2,…,j (i.e., crossing streets 1, 2,…,up to j), ξ=1,2, $x_{pWG\xi}$ is the position of a certain crossing street corner (see Fig. 1 in [**P5**]). The upper and lower bound in (3.5) determine rays that enter the side streets. Once the ray has been decided to couple the MS to the BS, formulas in [**P5**] for path

length, ground reflection angle, wall reflection angles in the main and perpendicular streets, etc., can be used to calculate the transfer function (3.1).

3.2.2. Modeling of radio wave propagation in perpendicular streets [**P6**]

The main investigated propagation mechanisms in [**P6**] are reflection and diffraction at vertical edges of street corners. Therefore, two groups of rays are considered in the model presented in [**P6**]. The first group of rays is the reflection-reflection rays (*RR*) group, which includes propagation paths via wall-wall reflections along the main and perpendicular street including or not the ground reflection. The second group of rays is the reflected-diffracted-reflected (*RDR*) rays group, which consists of rays that may be reflected along the main street and diffracted at street corners and may be reflected again along the NLOS perpendicular street with or without ground reflection. The rays are diffracted at all corners. Image theory and ray horizontal plane angle set membership criteria are utilized to find the possible coupling radio paths. The total channel transfer function of the above mentioned propagation mechanisms is given by

$$H_t = H_{RR} + H_{RDR} \tag{3.9}$$

where the H_{RR} and H_{RDR} is the total transfer function of the *RR* rays group and the *RDR* rays group. The following subsections summarize the derived expressions in [**P6**] for calculating the transfer function of each group.

3.2.2.1. Reflection –reflection rays group

The channel transfer function of *RR* ray group can be calculated by

$$H_{V,H} = \left(\frac{\lambda}{4\pi}\right) \sum_{i\equiv(S,m,g,u,n)} \left[f_B(\theta_i,\phi_i) f_M(\Theta_i,\Phi_i) \left(\Re^i_{V,H}\right)^g \left(R^{im}_{H,V}\right)^m \left(R^{in}_{H,V}\right)^n \frac{e^{-jkr_i}}{r_i} \right] \tag{3.10}$$

where ray *i* is represented by a set of five integers (*m*, *S*, *n*, *u* ,*g*), *m* and *n* are the wall reflection order in the main street and perpendicular street, respectively, *g* = 0,1 is the ground reflection order, $R^{im}_{H,V}$, and $R^{in}_{H,V}$ are the well-known Fresnel reflection coefficients for wall reflections in the main and perpendicular streets, respectively, with transmission in vertical and horizontal polarization of ray *i.* Also, with the notation shown in Figure 1 in [**P6**], *S* = 1, (2) for BS images with the first reflection on the wall $-y_1$ and $(w_1\text{-}y_1)$, respectively, and *u* = 1, (2) for MS images with the first reflection order on the wall $x\text{-}x_1$ and $(x\text{-}x_1+w_2)$, respectively.

Set membership criteria are defined in this work for the horizontal plane angles to distinguish the rays that couple the transmitter and receiver from those do not enter the perpendicular street or are lost in other streets before they arrive to the receiver. The checking criterion first determines the set of angles corresponding to rays that enter the perpendicular street. Then, it determines the set of angles correspond to rays that are lost in either side street before the perpendicular street or the rays that are lost in one of the parallel streets branched from the perpendicular street before they reach the MS. In order to check for rays that may enter the perpendicular street, the horizontal plane angle of ray *i* given by

$$\alpha_{i\_hplane} = \arctan\left(\frac{y-(-1)^S\left(\left(m+(-1)^S\Xi(m)\right)w_1 - 2(-1)^S\Xi(m)y_1\right)}{(-1)^u\left(\left(n+(-1)^u\Xi(n)\right)w_2 + (-1)^u\left(x-2\Xi(n)x_1\right)\right)} \right) \tag{3.11}$$

must satisfy the following set membership criteria:

$$\alpha_{i\_hplane} \in \begin{cases} \alpha : \alpha_{i\_lthr} < \alpha < \alpha_{i\_uthr} \cap \alpha \underset{S=2}{\overset{S=1}{\gtrless}} \alpha_{i\_c\eta}, & \forall m > 0 \\ \alpha : \alpha_{i\_lthr} < \alpha < \alpha_{i\_uthr}, & m = 0 \end{cases} \tag{3.12}$$

$$\alpha_{i\_(uthr,lthr,c\eta)} = \arctan\left(\frac{y_{c(\mu,\beta,\eta)} - (-1)^S \left(\left(m + (-1)^S \Xi(m) \right) w_1 - 2(-1)^S \Xi(m) y_1 \right)}{x_{c(\mu,\beta,\eta)}} \right) \tag{3.13}$$

where $\left(x_{c_i}, y_{c_i} \right)_{i=1 \text{ to } 4}$ are the positions of the corners at crossing streets between the BS and the perpendicular street, the subscripts $\mu = 4,(2)$, β=1,(3), and $\eta = 2,(1)$ are selected based on *S*=2,(1), respectively. Once the first set membership checking approves that the ray may enter the perpendicular street, it is necessary to check that the ray does not belong to rays that travel in any side street before the perpendicular street where the MS is located. The respective horizontal plane angle α_{i_hplane} of ray *i* must satisfy the set membership criterion given as

$$\alpha_{i\_hplane} \notin \bigcup_{p=1}^{J} \bigcup_{Q=\min(\aleph)}^{\max(\aleph)} \left\{ \alpha : \alpha_{pWGmQ\,1} \underset{S=1}{\overset{S=2}{\lesseqgtr}} \alpha \underset{S=1}{\overset{S=2}{\lesseqgtr}} \alpha_{pWGmQ\,2} \right\} \tag{3.14}$$

$$\alpha_{pWGmQ\xi} = \arctan\left(\frac{(-1)^S Q w_1 - y_1 - (-1)^S \left(\left(m + (-1)^S \Xi(m) \right) w_1 - 2(-1)^S \Xi(m) y_1 \right)}{x_{pWG\zeta}} \right) \tag{3.15}$$

$$\aleph = \left[1\ 2 \quad \ldots m \right] + \Xi(S) \tag{3.16}$$

where p = 1,2,…,J (*i.e.,* crossing streets before perpendicular street 1, 2,…, up to *J*), ξ=1,2, $G = S - (-1)^S \Xi(Q)$ and $x_{pWG\xi}$ is the position of a corner of a crossing street p (see Fig. 1 in [**P6**]). The upper and lower bound in (3.14) determine the rays that enter the side streets. Once the ray is determined to enter the perpendicular street, the last examination is to check that it does not travel into the parallel street branched from the perpendicular street before the MS. Thus, the horizontal plane angle α_{i_hplane} of the ray in the perpendicular street must satisfy the following set membership criterion:

$$\alpha_{i\_hplane} \notin \bigcup_{a=1}^{L} \bigcup_{\nu=1}^{n} \left\{ \alpha : \alpha_{aWAm\,\nu 2} < \alpha < \alpha_{aWAm\,\nu 1} \right\} \tag{3.17}$$

$$\alpha_{aWAm\nu\xi} = \arctan\left(\frac{y_{aWA\xi} - (-1)^S \left(\left(m + (-1)^S \Xi(m) \right) w_1 - 2(-1)^S \Xi(m) y_1 \right)}{(-1)^u \left(\nu w_2 - x_1 \right) + x} \right) \tag{3.18}$$

where a=1,2,…,L (*i.e.,* parallel streets 1, 2,…, up to L branching from the perpendicular street but before the location of the MS), ξ=1,2, $A = u - (-1)^u \Xi(\nu)$, $y_{aWA\xi}$ is the position of a certain crossing street corner (see Fig. 1 in [**P6**]). Once the ray has been decided to couple the MS to the BS, formulas in [**P6**] for path length, ground reflection angle, and wall reflection angles in the main and perpendicular streets can be used to calculate the transfer function (3.10).

3.2.2.2. Reflection-diffraction-reflection rays group

The channel transfer function of *RDR* rays group resulting from the four corners is

$$H_{RDR} = H_{C1} + H_{C2} + H_{C3} + H_{C4} \tag{3.19}$$

where H_{Ci} is the transfer function of rays due to corner *i*. The electric field for a ray path generated from the diffraction on the building corner is calculated by applying the uniform geometrical theory of diffraction. The UTD approach considers a single ray at a time and pieces together an overall received signal as a sum of all of the diffracted rays. The channel transfer function of a *RDR* ray can be calculated by

$$H_{V,H} = \left(\frac{\lambda}{4\pi}\right) \sum_{i=(m,S,n,u,g,Ci)} \left[f_B(\theta_i,\phi_i) f_M(\Theta_i,\Phi_i) \left(\Re^i_{V,H}\right)^g \left(R^{im}_{H,V}\right)^m \mathfrak{D}^i_{H,V} \left(R^{in}_{H,V}\right)^n \frac{1}{\sqrt{D_1 D_2 (D_1 + D_2)}} e^{-jk(D_1+D_2)} \right] \tag{3.20}$$

where $D_{1,2}$ are the distance from the BS and MS to the diffraction point on the building corner edge, respectively.

In order to determine the set of rays that connect the two terminals, set membership criteria must be fulfilled. The coupling radio paths have angular characteristics that must fulfill set membership criteria. In order to study these angular characteristics, the horizontal plane angle of each ray in both the main and perpendicular streets are used to check if the ray belongs to rays having certain set of angles. The horizontal plane angle of ray *i* in the main street is given by

$$\alpha_{ihp\_m} = \arctan\left(\frac{(-1)^S \left(\left(m + (-1)^S \Xi(m) \right) w_1 - 2(-1)^S \Xi(m) y_1 - Y_c \right)}{-X_c} \right) \tag{3.21}$$

Three sets of angle membership criteria must be examined to check for the coupling radio paths. First test is to ensure that the ray does not propagate in the side streets before the perpendicular street. To satisfy this condition, the following criterion must be fulfilled for each corner (H_{c1}-H_{c4}),

$$\alpha_{ihp\_m} \notin \bigcup_{p=1}^{J} \bigcup_{q=1}^{m} \left\{ \alpha : \alpha_{m-pWGq2} \underset{c2,c3}{\overset{c1,c4}{\lesseqgtr}} \alpha \underset{c2,c3}{\overset{c1,c4}{\lesseqgtr}} \alpha_{m-pWGq1} \right\} \tag{3.22}$$

$$\alpha_{m\_pWGq\xi} = \arctan\left(\frac{(-1)^S q w_1}{x_{pWG\xi} - X_c} \right) \tag{3.23}$$

where p=1,2,…,J (i.e., crossing streets before perpendicular street 1,2,…, up to J), $G = S - (-1)^S \Xi(q)$. The upper and lower bound in (3.22) determine the rays that enter the side streets. Once the ray is determined not to propagate into one of the side streets before the perpendicular street, the second examination is to check whether the concerned corner (c_1, c_2, c_3 or c_4) diverts the signal into the perpendicular street. First, the direct and multiple reflection rays from the BS that illuminate each corner are determined and after that the set of rays that each illuminated corner diverts in to the perpendicular street. The rays that couple the BS and its images to each illuminated corner must satisfy the angular criterion

$$\alpha_{ihp\_m} \in \left\{ \alpha : \alpha \underset{\substack{l=2,3 \\ k=1,1}}{\overset{\substack{l=1,4 \\ k=2,2}}{\gtrless}} \alpha_{c_l - c_k} \right\} \tag{3.24}$$

$$\alpha_{c_l - c_k} = \arctan\left(\frac{\mathrm{y}_{c_k} - y_{c_l}}{x_{c_k} - x_{c_l}} \right) \tag{3.25}$$

where $\left(x_{c_l}, y_{c_l}\right)$, $\left(x_{c_k}, y_{c_k}\right)$ are the co-ordinates of the *lth* or *kth* corners of the perpendicular streets. The rays that are diverted from corner *l* and propagate to the perpendicular street must satisfy the following criterion:

$$\alpha_{is\_hp} \in \left\{ \begin{array}{ll} \alpha : \alpha \underset{\substack{l=1,2 \\ k=4,4}}{\overset{\substack{l=3,4 \\ k=1,1}}{\gtrless}} \alpha_{c_l - c_k} & \forall y < y_1 \\ \alpha : \alpha \underset{\substack{l=3,4 \\ k=2,2}}{\overset{\substack{l=1,2 \\ k=3,3}}{\gtrless}} \alpha_{c_l - c_k}, & \forall y > \left(w_1 - y_1\right) \end{array} \right\} \tag{3.26}$$

where α_{is_hp} is the horizontal plane angle of the propagating ray in perpendicular street, which is utilized to check the set membership criterion. The horizontal plane angle is defined as

$$\alpha_{is\_hp} = \arctan\left(\frac{y - Y_c}{\left((-1)^u \left(\left(n + (-1)^u \Xi(n)\right) w_2 + (-1)^u \left(x - 2\Xi(n) x_1\right)\right) - X_c\right)} \right) \tag{3.27}$$

Once the ray has been determined to propagate in to the perpendicular street, the last check is to test that the ray does not propagate in to the parallel streets branched from the perpendicular street before the MS. The rays that couple the illuminated corner with the MS must satisfy the following set membership criterion:

$$\alpha_{is-hp} \notin \bigcup_{a=1}^{L} \bigcup_{b=1}^{n} \left\{ \begin{array}{ll} \alpha : \alpha_{s-aWAb1} \underset{c3,c4}{\overset{c1,c2}{\lesssim}} \alpha \underset{c3,c4}{\overset{c1,c2}{\lesssim}} \alpha_{s-aWAb2}, & \forall\ y \le y_1 \\ \alpha : \alpha_{s-aWAb1} \underset{c3,c4}{\overset{c1,c2}{\gtrsim}} \alpha \underset{c3,c4}{\overset{c1,c2}{\gtrsim}} \alpha_{s-aWAb2}, & \forall\ y \ge (w_1 - y_1) \end{array} \right\} \tag{3.28}$$

$$\alpha_{s\_aWAb} = \operatorname{atan}\left(\frac{y_{aWA\xi} - Y_c}{(-)^u b w_2} \right) \tag{3.29}$$

where a=1,2,…,T (i.e., crossing streets before the perpendicular street 1,2,…, upto L), ξ=1,2, $A = u - (-1)^u \Xi(b+1)$ and $y_{aWA\xi}$ is the position of a certain crossing street corner (see Fig. 1 in [**P6**]). The upper and lower bound in (3.28) determine the rays that enter the parallel streets before the MS. Once the ray has been decided to couple the MS to the BS, formulas in [**P6**] for path length, ground

reflection angle, wall reflection angles in the main and perpendicular streets, etc., can be used to calculate the transfer function (3.20).

The proposed models of radio waves propagation in the main street in [**P5**] and in the perpendicular street in [**P6**] are ray based models and have the same accuracy of image based ray tracing. They can be used for propagation prediction in the main and perpendicular street. They can also be used to characterize radio channels of these street types and study propagation problems in the microcellular environment. Samples of these applications are presented in Section 4.2 of this thesis summary.

3.3. Secondary Source Modeling Approach [P7]

Planning tools for future mobile communications systems for microcells require very fast and accurate path loss models to estimate the coverage. In addition, algorithm testing requires path loss models that are separate from fading distributions. In such applications, usually fading is added, as a separate term with a specific distribution for either slow or fast fading, to the distance dependent part. The model presented in Section 3.2 can provide path loss together with multipath interference, which causes fading that is superimposed on dominant rays. The dominant path gain plus multipath interference compose the path loss and fading pattern. The dominant path gain depends on the dominant propagation mechanism. In perpendicular streets, the reflection process is dominant just after the disappearance of the LOS component for some distance in the street, then scattering is dominant for distance in the middle shadow region of the street. In the deep shadow region, the diffraction process is dominant. In order just to determine the path loss (i.e., dominant mechanisms) without multipath interference, a very fast approach (i.e., faster than that in Section 3.2) is needed for the above applications.

In this thesis work in [**P7**], a principle for modeling path loss in perpendicular street is presented which is an extension to the work presented in [111] for path loss in parallel streets. The model is for the path loss of radio waves propagation into a perpendicular street. The model is given in a mathematical closed form, which takes into account the information about the position of the BS and the MS in a microcellular environment. The proposed technique is based on the secondary source principle, which maps the NLOS propagation problem to the LOS propagation problem. The mathematical formulation of the model is based on the principle that the power leakage into the perpendicular street is regarded as the power of a secondary source for the propagation of radio waves into the side street. In order to determine the dominant corner for the diffraction process, Figure 3.2 shows effect of each corner on the received power at the MS along a perpendicular street. Each corner can be considered as a secondary source of the power that reaches the MS. It is clear that the power diffracted by corner C3 is dominating. This corner will divert signals into the perpendicular street and dominates the propagation mechanisms in deep shadow region. If the MS is in the opposite direction of the street (i.e., north part), diffraction due to corner C4 is the dominant. It is more acceptable from physics point of view that the secondary source is located at the edge of the building corner whose two sides can be seen by the BS and the MS, e.g.., corner C3 in Figure 3.2. The assumption that main energy arrives at the MS in the perpendicular street from a dominant source has been confirmed recently [87] by analysis of wideband directional measurement results. The measurement result allows the investigation of DoA of multipath components in angular domain. The investigation shows that the main signal arrives from dominant directions that correspond to the locations of building corners at the street junction. Figure 3.3 shows the azimuth DoA distribution of the multipath components at the MS along route G-H (see inserted map in Figure 3.3). Since the MS travels from point G to point H and the zero direction is the traveling direction, we can see that the main directions of arrivals of multipath components are around zero angle direction in the range of about the first 100 m. Once the MS gets into the NLOS again, arrival angles of the MPC start to arrive mainly from the back of the traveling direction of the MS, which is around 180^{o}. From this analysis, we can observe that the main energy arrives the MS from dominant secondary sources. Figure 3.4 shows comparison between the measured path gain along route G-H and that

obtained by the model presented in [**P7**] in the NLOS sections of the route G-H. Clearly good agreement can be seen. This model has been selected by the propagation research group at Communication Research Center (CRC) in Canada [89-90]. The model has given the best agreement with measurements results at 1.8 GHz on 15 different trajectories from streets within 5 city blocks of the transmitter sites. The rms variations of the comparison between experimentally-determined local means (determined for over 40 wavelengths) with respect to the model have ranged between 2.5 dB to 9 dB.

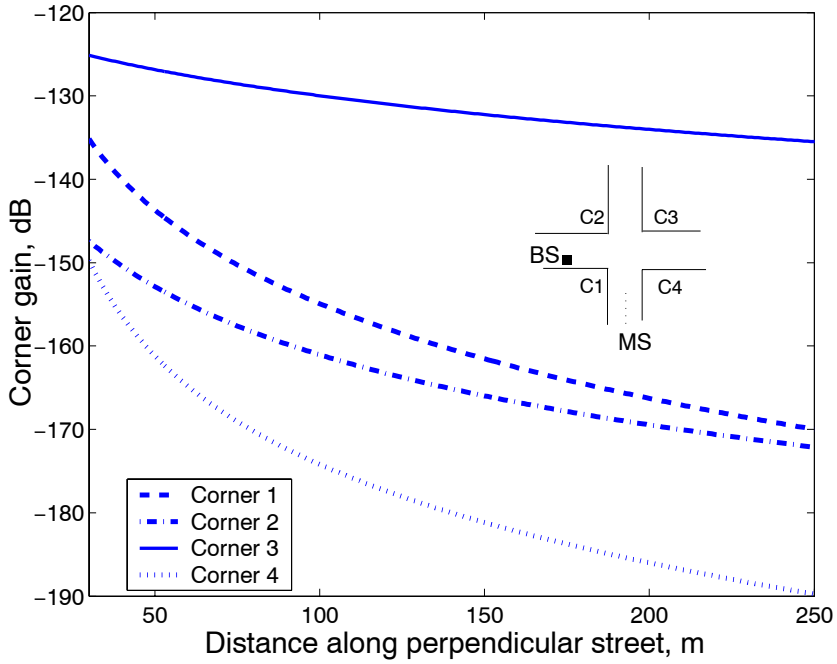

Figure 3.2. Building corners as secondary sources.

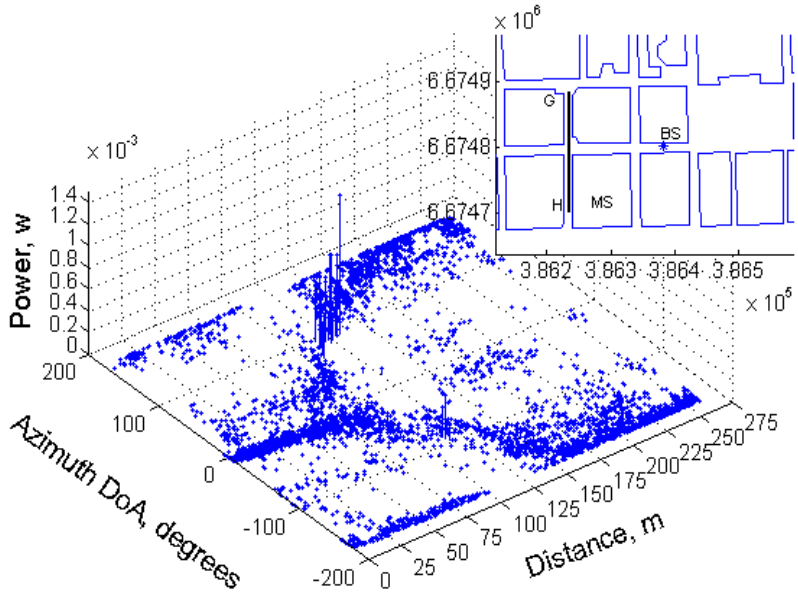

Figure 3.3. Azimuth power spectra in perpendicular street.

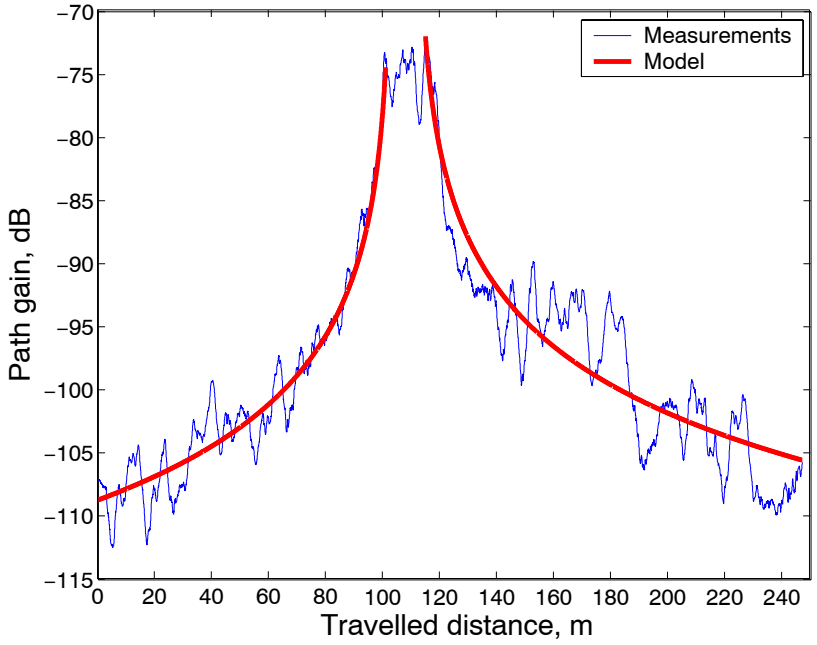

Figure 3.4. Path gain along route G-H.

3.4. Influence of Corner Shape on Accuracy of Propagation Prediction [P1]

The influence of the database inaccuracy on path loss predictions has been investigated in terms of details of each building block, especially openings between buildings and the location of building corners. Building corners are usually modeled as right angle wedges for prediction of diffracted field due to these corners. In this thesis work, the emphasis is on the shape of the building corners and their electrical properties. Results in [**P1**] show that a building corner having a reflecting flat surface as shown in Figure 1 in [**P1**], instead of a sharp corner, results in good agreement with measurement results. The flat surface reflects the signal into a long segment along a perpendicular street. Modeling the corner by a right angle wedge implies that the corner acts as a diffracting edge, which results in predicted signal amplitude that is smaller than the measured one, as seen in Figure 10(a) in [**P1**]. The reflecting surface of the corner is seen in Figure 1 in [**P1**] to consist largely of glass. For the low base station antennas discussed in [**P1**], it is the doors and window above them that are responsible for the reflections. If the reflection coefficient for this wall computed with ε_r =6, used also for all other walls, the prediction highly overestimates the signal, as seen in Figure 10(a) in [**P1**]. Selecting a lower value of permittivity only for this surface and keeping other surfaces with ε_r = 6, is seen to give better agreement with measurements. The rms delay spread shown in Figure 10(b) in [**P1**] is also seen to be better predicted using the correct corner shape and ε_r = 2. Predictions made with the right angle wedge shape give a much higher delay spread in the region from 20 m to 70 m, while predictions made with ε_r = 6 are generally too low. From the results presented in [**P1**] it can be seen that the corner shape has clear influence on the prediction of the received power and the rms delay spread. It is seen that the influence on the prediction of the received power is greater than on the prediction of the rms delay spread. This result emphasizes the importance of the accuracy of the shape of the building corners and their electrical properties for accurate predictions. It is also found that the position of the corner of accurate shape is very important. Since the corner acts as a reflector, inaccuracy of its position relative to other corners at the intersection may lead to the prediction of high reflected power along the perpendicular street.

4. Characterization of Radio Channels

4.1. Introduction

The successful design of wireless communication systems requires detailed understanding of propagation channels. Knowledge of channel characteristics enables reaching optimum trade off between system performance and complexity. Radio channel characterization is important for both network planning and radio interface design of communication systems. Two types of characterizations are generally considered that termed as large-scale and small-scale characteristics. The small-scale parameters usually provide statistical information on local field variations and this, in turn, leads to the calculation of important parameters that help to e.g., improve receiver designs and to combat or utilize the multipath phenomena. Characterizing the channel in terms of coverage and interference analysis, *i.e.,* large-scale characteristics, is important for network planning. Characterizing the channels in terms of delay spread, angular spreads, coherence bandwidth, finger characteristics, correlation properties, etc. is important for successful receiver design. Multipath components (MPC) can be characterized by their amplitude, delay, angle of arrival and departure, Doppler-frequency, and polarization. The detailed information leads to understanding of propagation mechanisms and their importance for radio wave propagation modeling and may answer to questions like: what is the dominant propagation mechanism in the propagation environment? Is it reflection, diffraction or scattering? What is more important: over-the-roof or around-corner diffraction in outdoor urban environment for different base station (BS) antenna heights? The detailed information of the MPC also leads to the development of more realistic spatial channel models needed for testing algorithms for smart antennas or MIMO systems [91]-[93]. Radio channels can be characterized based on theoretical models or measurement results. In the following sections, models presented in [**P5**] and [**P6**] are used to characterize mircocellular radio channels. Wideband measurement at 2 GHz results are analyzed to characterize radio channels in terms of Rake finger characteristics, orthogonal factor for W-CDMA downlink channel, delay and direction spread, and (dis-) similarity between multipath components in delay and angular domains.

4.2. Model-based Characterization of Radio Channel

Ray-based models can be used as a powerful and efficient tool, which might be considered as an alternative to measurements to enable statement about radio channel characteristics in delay, angular and Doppler domains with different polarizations. The models in [**P5**] and [**P6**] can be used to characterize radio channels in the main and perpendicular streets. The characterization can be done for vertical and horizontal polarizations. The polarization dependence of multipath components in the main street has been studied by the author of this thesis in [94], [95]. It has been shown that the power delay profiles of vertical and horizontal polarization transmissions are similar at distances close to the base station but are considerably different at large distance separation. It has been shown that the vertically polarized narrowband signals suffer higher fast fading than that of horizontally polarized ones. This might be explained as follows: for vertical (or horizontal) polarization transmission, the electric field is in parallel (or perpendicular) with respect to the building wall. The perpendicular polarized field suffers more loss in multiple reflections. So, multipath interference, which causes fast fading, will be more significant for vertically polarized transmission. The model in [**P5**] has been used in [96] by the author to investigate a proposed technique for the control of propagation characteristics by utilizing transmitting array antennas at the BS. The propagation control technique can be used for interference reduction between neighbouring cells and controlling the coverage area size (e.g., controlling the propagation slope) [96]. The models can also be used to study propagation problems such as mitigating channel impairments. The model in [**P5**] is used in [97] to characterize space and frequency diversity in the main street for different street widths. It is found that a transversal configuration, *i.e.,* where two spaced antennas are placed perpendicular to the main street, is less sensitive to widths of streets than

the longitudinal configuration, where two spaced antennas are placed parallel to the main street. Spatial diversity gain is higher for the transversal configuration than that obtained with the longitudinal separation, which may indicate to having possible higher MIMO capacity with transversal configuration. Spaced-frequency envelope correlations, it is the correlation of the two received signals as channel responses of two transmitted sinusoidal signals, decreases slowly with increasing frequency separation. Spaced-frequency correlation also decreases with increasing street width. Frequency diversity can be obtained by large separation in frequency. Frequency diversity gain changes with increasing street width. The model in [**P5**] has also been used in [112] for studying MIMO capacity in the main street of a street grid under different conditions.

4.3. Channel Characterization for Rake Receiver Design [P8]-[P10]

In CDMA systems using Rake receivers, correlator branches or Rake 'fingers' are used to capture part of the signal energy. These fingers are assigned to different time delay slots in the channel impulse response and utilize the signal energy present in those time delay bins. The width of the delay bins is directly related to bandwidth. In order to optimize the Rake receiver design, channels must be characterized in a way that provides the required information. This channel characterization should include the number of useful fingers, the power contribution of each finger, the finger life distance. Since the receiver system reallocates Rake receiver fingers dynamically, system designers require the knowledge of the number of the effective individual multipaths. In [**P8**] and [**P9**], measurement results obtained in microcells (*i.e.,* antennas are below buildings rooftops) and small cell (*i.e.,* the BS antenna above rooftop with distance less than 1 km) are analyzed in terms of finger characteristics. In [**P8**], the receiver has 32 dual polarized antenna elements in a spherical array, while in [**P9**], the receiver has a single directional antenna. Every finger, whose mean power is above a certain threshold (i.e., 13 dB in [**P9**]) below the peak value of the considered power delay profile, is considered as an active finger. The influence of bandwidth on the distinguished number of fingers is considered in more details in [**P8**], where results for bandwidths of 5, 10, 20, and 30 MHz are presented. The number of active fingers for different bandwidths is analyzed for both microcells [**P8**] and small cells [**P9**]. The number of distinct active fingers increases with bandwidth since the path time resolution increases and chip duration decreases. In [**P9**], the median value of the number of active fingers for bandwidths of 5 and 30 MHz is 3 and 5, respectively, while their corresponding values in [**P8**] are 4 and 10, respectively. Having 32 directional antennas distributed around a sphere allow signal detection from all directions.

The other parameter that is important to consider for the Rake receiver design is the finger life distance. For frequency selective fading channels, from the viewpoint of acquisition, the existence of multipaths implies that there exist more than one in-phase (synchro) cells, for a channel with L distinguishable paths there will be L in-phase cells. The acquisition process is supposed to find the delay positions of all of them, and the tracking step is expected to track all of them. Thus, detailed characterization of the propagation channel in the path domain is important for the design of synchronization part of wideband DS-CDMA systems. Two important issues are the number of active fingers and their lifetimes, *i.e.,* how long the system will be in synchronism. In [**P9**] and [**P10**], results for finger life distance for small cells and microcells, respectively, are presented. In [**P9**], for 5 and 30 MHz bandwidth, the median finger life distance of the second and third fingers are 2 and 1 m, respectively, while their corresponding values in microcell [**P10**] are 2 and 1.5 m for a perpendicular street and 3 and 0.5 for a parallel street.

4.4. Characterization of Orthogonality Factor for W-CDMA Downlink Channel

The demand for multimedia services in mobile communications is expected to require more capacity in W-CDMA downlink. In downlink W-CDMA systems, users in one cell are separated by means of

synchronized orthogonal codes [98]. When radio channels have no time dispersion, the own cell interference is eliminated after despreading. However, the orthogonality is partly destroyed when the channel is time dispersive because the delayed versions of the orthogonal characterization codes are not orthogonal. The orthogonality factor (OF) has been widely introduced and accepted as a measure of the degree of the orthogonality between own cell signals received by a particular user. Results in [100], [103], [104] are based on simulations. However, this thesis results are based on wideband measurements. In the downlink, the energy per bit to interference plus noise ratio (ρ) after Rake combining for a particular user is a function of OF [99]-[103] as

$$\rho = \frac{R_c}{R_b} \frac{P_{user}}{P_{own}(1-\alpha) + P_{other} + P_{noise}} \tag{4.1}$$

where R_c is chip rate, R_b is bit rate, P_{user} is the received power of the desired signal, P_{own} is the total power from own cell BS, P_{other} is the total received power from other BSs, P_{noise} is the thermal noise, and α is the OF. The term (1-α) is termed as the multipath loss factor of the radio channel [104]. The importance of the OF depends on the interference ratio $G = P_{own}/(P_{other} + P_{noise})$. Hence, for $G << 1$ the OF becomes less important for the value of ρ, while ρ becomes dependent on the OF for $G >> 1$. An approximate formula for the OF is presented in [104] for the case where it is averaged over the radio channel and $G >> 1$, *i.e.,*

$$\alpha = 1 - \left[\sum_{n=1}^{N} \frac{\beta_n}{\sum_{l=1, l \neq n}^{L} \beta_l} \right]^{-1} \tag{4.2}$$

where β_l is the power of finger *l* where fingers are ordered in power (the first finger has the strongest power and so on), *L* is the total number of fingers, *N* is selected number of fingers that can capture certain percentage (i.e., 95% in this work) of total power. The average OF, α, is only dependent on power of fingers and not dependent on the temporal behavior. The OF value for the 3G system of 5 MHz bandwidth is between 0.4 and 0.9 in multipath channels [98], [99]. The enhanced-IMT2000 is expected to work with bandwidth higher than 5 MHz. The proposed bandwidths are 10 and 20 MHz. This section presents the influence of bandwidth on the OF. The cumulative distribution function (cdf) of the variation of the OF extracted from measurement data along routes G-H and I-J in microcellular environment shown in Figure 4.1 are presented in Figure 4.2 for different bandwidths. The measurement system has a bandwidth of 30 MHz. The lower bandwidths are obtained by filtering down to the desired lower bandwidth. Statistical parameters of OF are given in Table 4.1. It can be seen that the mean and median of the OF along routes G-H and I-J are about 0.4 and 0.5 for the case when the bandwidth is 5 MHz. It can be seen from the curves in Figure 4.2 and Table 4.1 that as the bandwidth increases the OF decrease which indicates to more orthogonality destruction. This is due to more distinguished multipaths with higher bandwidths. The more there are multipaths the lower is the OF. Thus, the currently used values of OF, i.e., 0.6, [99], for the W-CDMA system of 5 MHz bandwidth, are unlikely to be reliable for higher bandwidth as they may overestimate the capacity of the system.

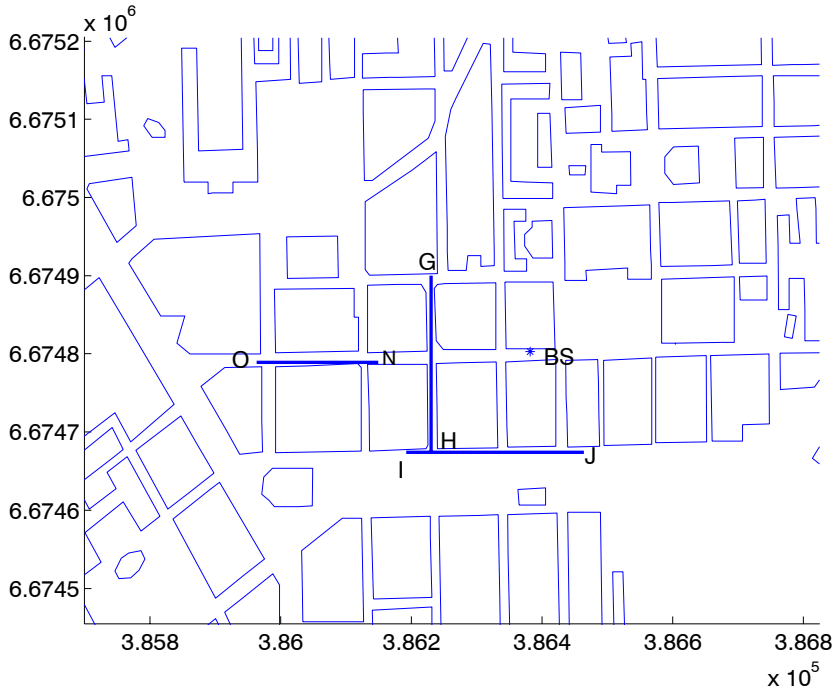

Figure 4.1. Propagation environment.

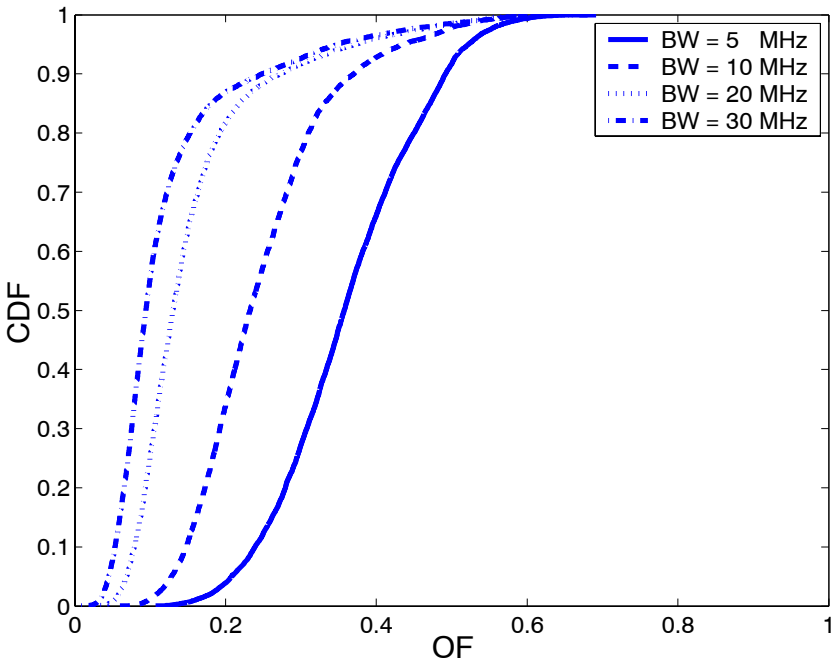

(a)

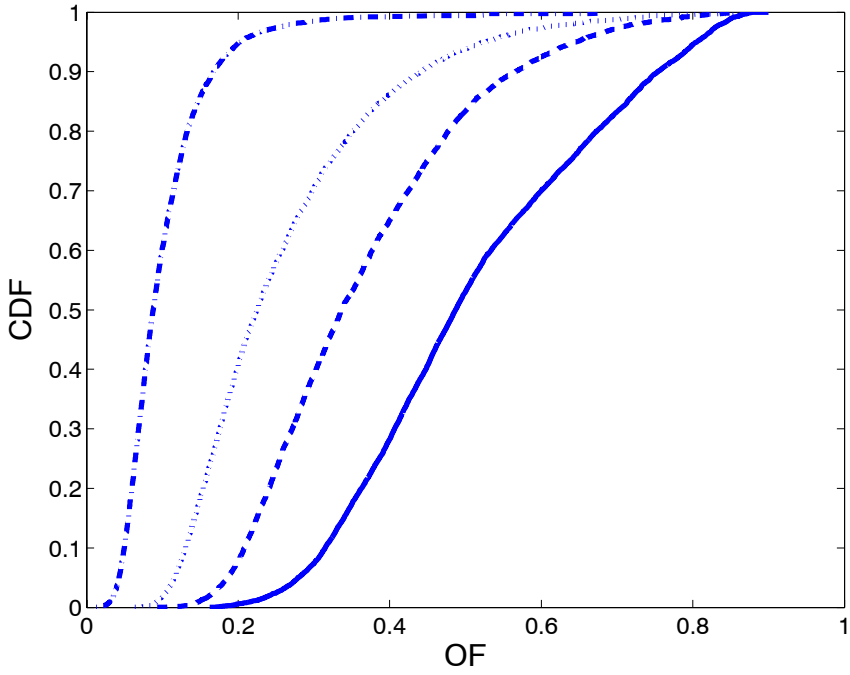

(b)

Figure 4.2. Cumulative distribution function of orthogonality factor in microcellular environment. (a) Route G-H. (b) Route I-J.

Table 4.1. Statistical parameters of orthogonality factor in routes G-H and I-J.

	Min				Max				Std			
BW (MHz)	5	10	20	30	5	10	20	30	5	10	20	30
Route G-H	0.11	0.06	0.02	0.01	0.69	0.63	0.66	0.68	0.1	0.09	0.09	0.1
Route I-J	0.17	0.13	0.09	0.06	0.9	0.88	0.86	0.68	0.16	0.14	0.13	0.06
	Mean				Median							
	0.36	0.25	0.16	0.13	0.36	0.23	0.13	0.09				
	0.51	0.36	0.26	0.10	0.49	0.34	0.22	0.09				

4.5. Characterization of Dispersion Metric Parameters

The design of advanced broadband wireless communication systems requires efficient understanding of wideband radio channels. The potential application of adaptive antennas leads to the angular representation of the spatial domain. The transmitted signals disperse in delay and spatial domains before they reach the receiver. The adaptive antennas and wideband radio channels necessitate spatial and temporal processing at the receiver. Some metrics are used to characterize each domain dispersion. The most common dispersion metric in delay domain is the root mean square (rms) time delay spread (DS) which is defined as the square root of the second-order central moment of power delay profile. Various definitions of addressing appropriate parameters characterizing azimuthal dispersion in the case of azimuth propagation have been published [105]-[107]. The adopted definition of angular spread (AS) in this thesis work is the one presented in [107], which is termed as direction spread. The mean vector direction of arrival in [107] is expressed in [108] by

$$\overline{\underline{\nu}^{(j)}} = \frac{\sum_m \left|A_m^{(j)}\right|^2 \underline{\nu}_m^{(j)}}{\sum_m \left|A_m^{(j)}\right|^2} \tag{4.3}$$

and the direction spread is given in [108] as

$$AS^{(j)} = \frac{180}{\pi}\sqrt{1-\left|\overline{\underline{\nu}^{(j)}}\right|^2} \,. \tag{4.4}$$

where A_m is the amplitude of ray m with unit vector direction $\underline{\nu}_m$. This definition extends the concept of the center of gravity and square root of second central moment to a unit vector pointing toward the direction of arrival of the incident ray to obtain the direction spread of the radio channel. In order to characterize the dispersion in microcellular environment, measured data along routes shown in Figure 4.1 are processed for calculating DS and AS for BS antenna height of 3 m and 13 m. Figures 4.3 and 4.4 represent the CDF of the AS and DS, respectively, for routes N-O, G-H, and I-J for both BS antenna heights. It is clear that the AS is affected by different antenna heights in the LOS scenario, while no significant change in the CDF with antenna height is seen for NLOS perpendicular street, i.e., G-H, route and parallel street, i.e., I-J, route. The influence of the antenna height on the DS is higher for LOS scenarios than the NLOS streets. One important parameter is the correlation between the AS and DS. Table 4.2 shows the correlation coefficient for routes N-O, G-H, and I-J for both antenna heights. High correlation coefficient can be seen for the LOS cases with two antenna heights and low correlation can be noticed for NLOS streets at both heights of the BS antenna.

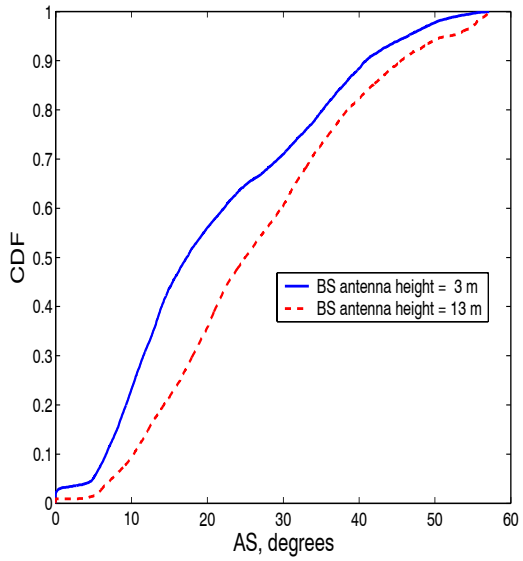

(a)

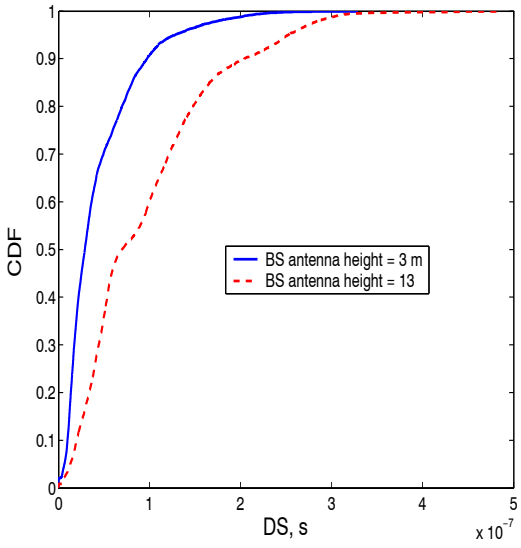

(a)

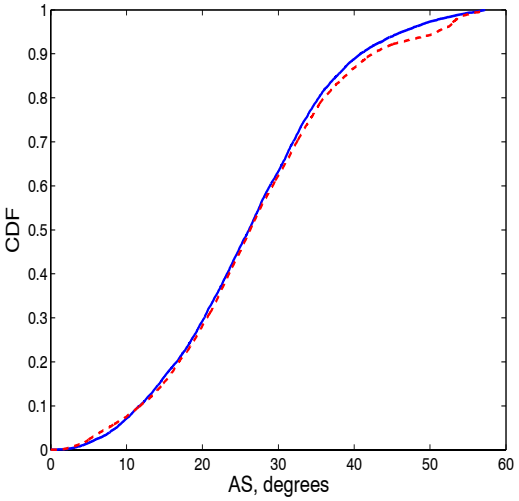

(b)

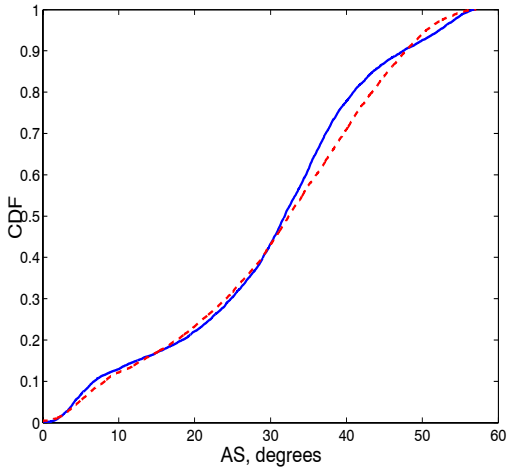

(c)

Figure 4.3. Cumulative distribution function of rms angular spread. a) Route N-O. (b) Route G-H. (c) Route I-J.

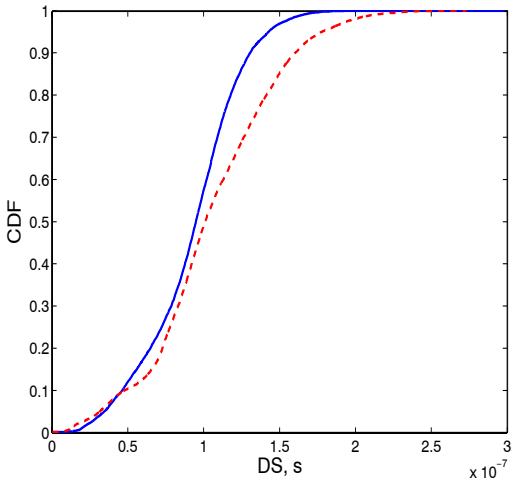

(b)

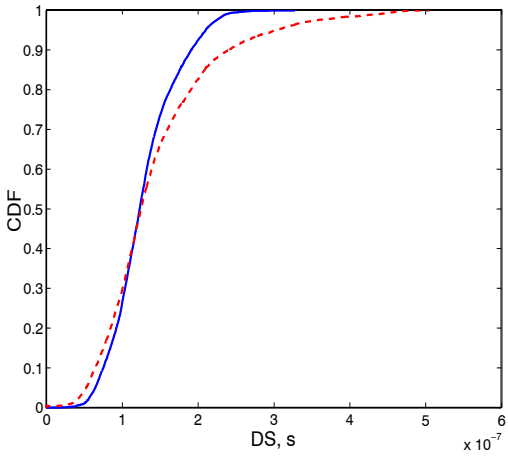

(c)

Figure 4.4. Cumulative distribution function of rms delay spread. (a) Route N-O. (b) Route G-H. (c) Route I-J.

Table 4.2. Correlation coefficient between AS and DS.

	BS antenna height	
	3 m	13 m
Route N-O	0.753	0.749
Route G-H	-0.192	-0.157
Route I-J	0.292	0.137

4.6. Characterization of Separation Distance of Multipath Components

The distinction between different propagation paths can be done by their delay, angle of arrival, angle of departure and Doppler-frequency. This also yields a possibility to have a measure that calculates a grade of (dis-) similarity between different multipath components. For instance, if two different multipath components (MPC) arrive in close times of arrival and clearly from different directions of arrival, the measure will result similarity in delay domain and dissimilarity in angular domain. The detailed characterization gives more insight view about MPC clustering of the channel and may answer questions like if multiple multipath clusters exist or not and what is the rate of appearance? Does clustering take place in delay or angular domains or both? and how many of them in each domain if there are any? How much power do they carry? and if there are two or more clusters how much are they separated? Clustering is getting more attention for spatial channel modeling. In order to develop an algorithm for extracting multipath cluster characteristics, the first step is development of (dis-) similiarity measure suitable for domains of multipath channels. The proposed measure utilizes the concept of multipath separation distance that has appeared in [109]. This thesis work introduces the concept of distance function as a measure of the (dis-) similarity between MPC. This concept has been developed to provide a formal description for measuring distance between two points in a vector space. The introduced concept and distance functions for multipath separation distance make the results in [109] as a special case of it. We propose them for multipath separation distance and discuss it as a step toward development of algorithm for extracting cluster characteristics of multipath radio channels from a huge amount of measurement results instead of the currently used manual approach. Many distance functions have been used in different applications, machine learning, neural networks and statistics [110]. When applied to multi-dimensional spaces, many of these distance functions are based on the differences between the values of each dimension. Following the same approach for characterizing multipath component separation, these functions may be applied in the MPC characterizing domain *j*: delay, Doppler, and angular both departure and arrivals. The most common of such distance functions is the Minkowsky function [110]:

$$d_j(X,Y) = \left(\sum_{i=1}^{n} |x_i - y_i|^p \right)^{\frac{1}{p}} \tag{4.3}$$

where the value p, positive integer number, enables the representation of several common distance functions, such as $p = 1$ comes to the Manhattan (*i.e.,* city block) distance, $p = 2$ gives the Euclidian distance, and $p = \infty$ is the Chebychev distance functions [110]. Data of each MPC in delay and Doppler domains are given in scalar values, *i.e.,* $n = 1$ in (4.3), while unit direction vectors ($[\sin\theta_k \cos\phi_k \quad \sin\theta_k \sin\phi_k \quad \cos\theta_k]$), either departure from transmitter or arrival at receiver, represents data in angular domain, *i.e.,* $n = 3$ in (4.3). We use, in later computation results, the Euclidian distance, $p = 2$, as a measure of distance between multipath components. For delay and Doppler domains, n=1, Euclidian, Manhattan, and Cheybechev distances give the same results. Thus, delay-, Doppler frequency difference distances between ray k and ray l is $|\tau_k - \tau_l|$, $|\upsilon_k - \upsilon_l|$, respectively. Available N domains are combined in one figure of merit as multipath separating distance (*MSD*) of paths k and l using the Euclidean distance, i.e., $p = 2$, as [109]:

$$MSD_{kl} = \sqrt{\sum_{j=1}^{N} d_j^2} \tag{4.4}$$

where d_j, which has different units for different dimensions, is the difference distance in dimension j calculated by (4.3). The MSD_{kl} is calculated for all pairs of paths for every MS location. At least two comments on (4.4) necessitate normalization in (4.3): (a) summation of different dimensions of different units, (b) the weakness of the basic Euclidian distances function is that if one of the input

dimensions has a relatively large range, then it can overpower other dimensions. Normalization usually takes place by dividing the distance of every dimension by its range. So, that the distance is in the approximate range 0…1, the maximum distance is unity and the minimum distance is zero. Thus, the *MSD* in (4.4) ranges from zero to the square root of the number of processed dimensions. With the analogy to the mean excess delay and rms delay spread, we propose the mean and rms of power-weighted *MSD* spread denoted as MSD_μ and MSD_σ, respectively, as follows:

$$MSD_\mu = \frac{\sum_{k=1}^{n}\sum_{l=k+1}^{n-1} MSD_{k,l} P_{k,l}}{\sum_{k=1}^{n}\sum_{l=k+1}^{n-1} P_{k,l}} \tag{4.5}$$

$$MSD_\sigma = \sqrt{\frac{\sum_{k=1}^{n}\sum_{l=k+1}^{n-1} \left(MSD_{k,l} - MSD_\mu\right)^2 P_{k,l}}{\sum_{k=1}^{n}\sum_{l=k+1}^{n-1} P_{k,l}}} \tag{4.6}$$

where n is number of *MPC* and $P_{k,l} = \sqrt{P_k P_l}$ is the cross-power of paths k and l reduces the effect of low power components. It is clear that $MSD_{k,k} = 0$. These parameters may help in getting information about clustering of MPC, number of dominant paths, and may also support optimizing beamforming or diversity processing. Power weighting of $MSD_{k,l}$ by their corresponding power $P_{k,l}$ results in information about the paths of high power that might be useful and possible to separate. These paths will have high power-weighted *MSD* values to separate. In [87], the separation distance of multipath components in microcellular environment is analyzed for main, perpendicular, and parallel streets, see Figure 4.1. Figure 4.5 shows the spatial variation of the power delay profile (PDP) at the MS along a LOS scenario, route N-O in Figure 4.1. All presented delays in this work are not absolute. Figure 4.6 depicts the spatial variant power azimuth profile. The measurement data in Figure 4.5 and 4.6 are used to calculate the *MSD*, MSD_μ, and MSD_σ. Figure 4.7 shows the complementary cumulative distribution function (ccdf) and the insert represents a histogram of the percentages of intervals of steps of 0.1 of *MSD* of MPC at the MS. This figure represents the separation distance in delay, angular and both combined domains. One can see that the delay *MSDs* have high frequency of occurrences for short distances (*i.e.,* 0.1) and the percentage decreases considerably with higher distance. This is expected since multipath components are close to each other in delay domain for short excess delay as can be seen in Figure 4.5. The excess delay width with respect to the range of the delay of multipath components (*i.e.,* length of the impulse response) is small. It should be noted that the separated large delay *MSDs* indicate the presence of separated MPC clusters in delay domain. Figure 4.7 shows also the angle of arrival (AoA) *MSDs*. The AoA *MSDs* include elevation angle information. The AoA *MSDs* have considerable percentage of short and long distances. The small values of AoA *MSDs* indicate arrivals of MPC close in angular domain while long distances (0.9-1) indicate to the arrivals of MPC from almost opposite directions to each other. Figure 4.7 also presents the *MSD* for both domains. It is clear that considering more domains we get higher values of *MSD*, which indicate superiority of processing more domains in finding separated multipath components. The flattening in the ccdf curve indicates scarcely available components of *MSD* in that region, which can be seen in the histogram insert in Figure 4.7. Figures 4.8 and 4.9 show MSD_μ and MSD_σ of the MPC, respectively, at the MS along route N-O. It can be seen that the MSD_μ of the delay *MSD* have low values indicating that mean of *MSDs* of components having significant power are close to each others in the delay domain with small variation in the MSD_σ values, which indicate to large number of multipath components are in one main cluster in delay domain. However, the results in the angular domain show that the MSD_μ values

are for the MPCs arrive almost opposite to each other with small MSD_σ values, which indicate to two main clusters almost opposite to each in angular domain. Considering both domains, one can see that the MSD_μ and MSD_σ have high values indicating that high separation distance can be achieved when delay and angular domains are combined.

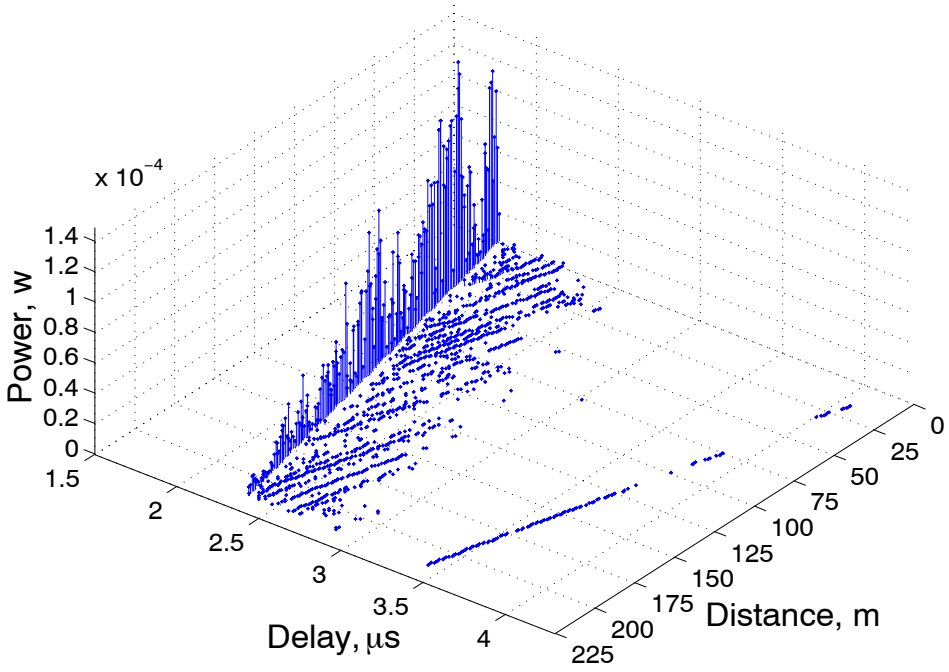

Figure 4.5. Spatial variant power delay profiles.

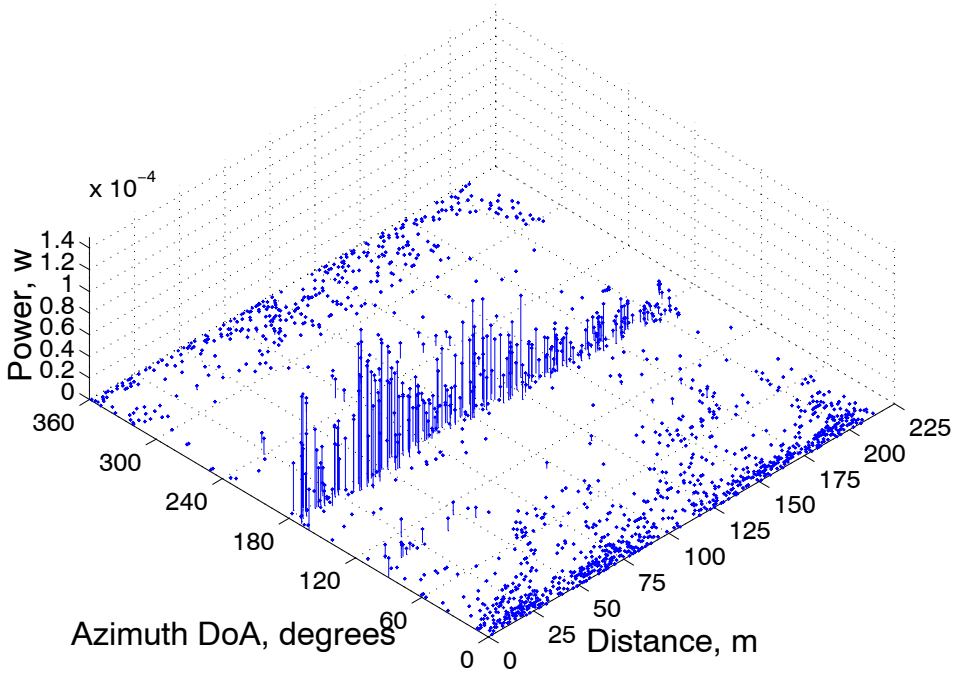

Figure 4.6. Spatial variant of power azimuth profiles.

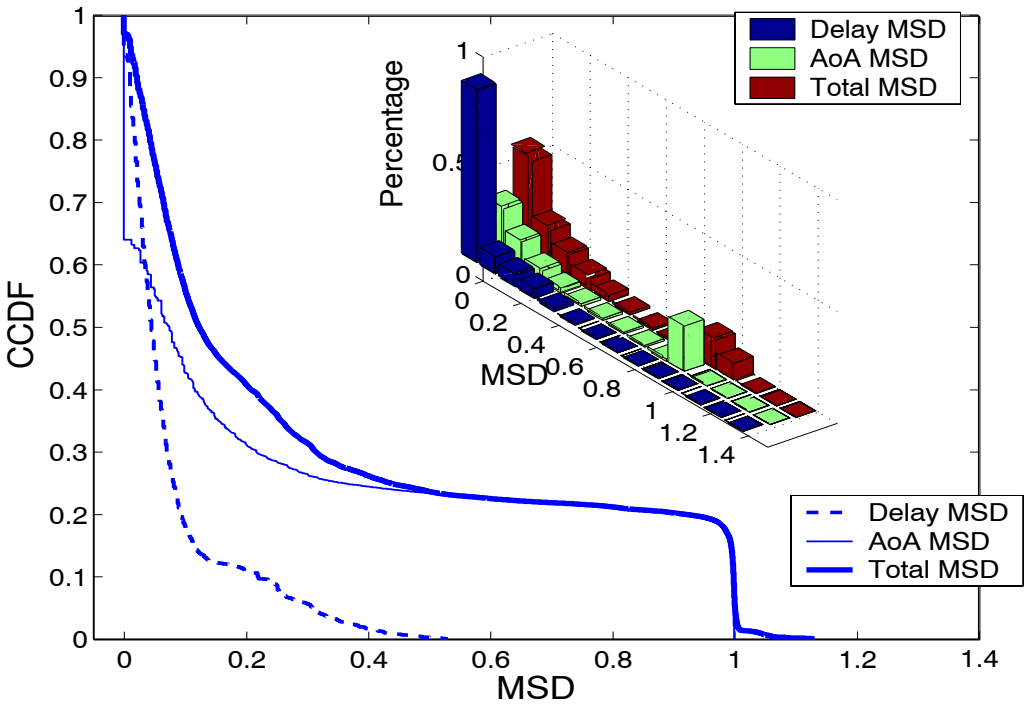

Figure 4.7. Ccdf and histogram of MSD.

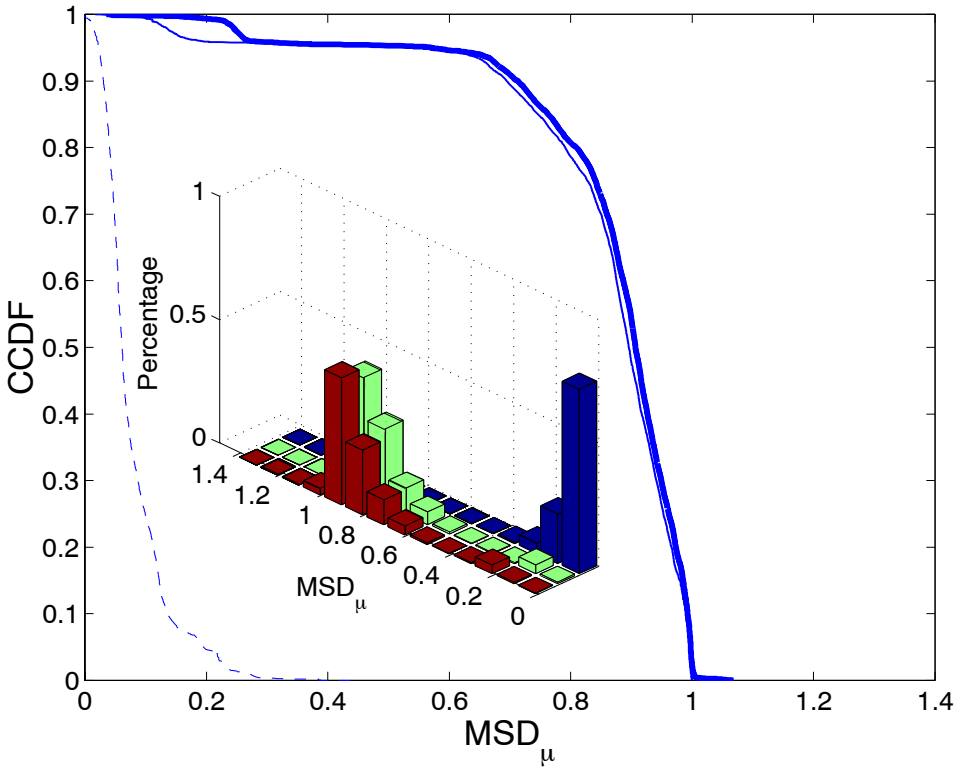

Figure 4.8. Ccdf and histogram of MSD_μ.

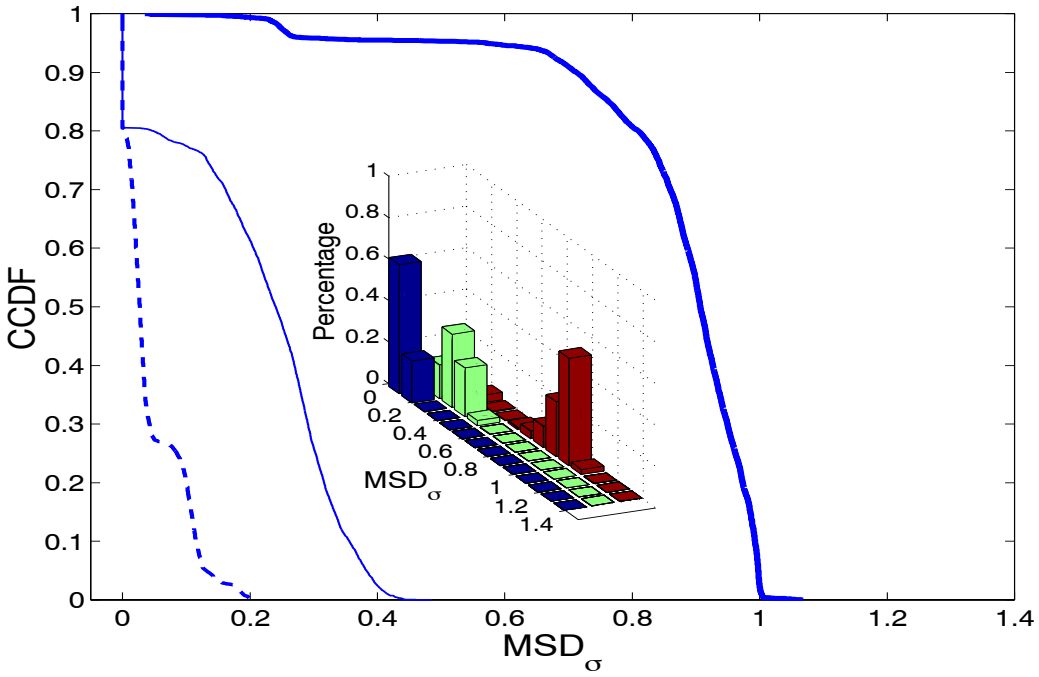

Figure 4.9. Ccdf and histogram of MSD$_\sigma$.

5. Summary of Publications

Paper [**P1**] presents the influence of diffraction coefficient and corner shape on ray prediction of received power and delay spread. Building corners can be represented as hollow wedges. The field beyond such corners is higher than that of solid wedges, which is the type usually assumed in outdoor propagation modeling. This paper compares ray-tracing predictions to measurements and shows the need for a diffraction coefficient having larger values than that obtained by the commonly used heuristic diffraction coefficient. A new heuristic diffraction coefficient is proposed that has higher diffracted field strength in the deep shadow region and in the region between the two shadow boundaries. The ray tracing with the proposed diffraction coefficient shows better agreement with measurements compared to the commonly used heuristic diffraction coefficient. The influence of building shape near the corner and its electrical properties on the ray tracing predictions show that they have an important role in accurately predicting both received power and delay spread.

Paper [**P2**] shows that the commonly used diffraction coefficient in propagation prediction tools may lead to inaccurate results. A new heuristic diffraction coefficient is proposed for impenetrable wedges. It introduces modified reflection coefficient that was inferred from suitable formulation of the Maliuzhinets' solution as a multiplication factor that multiplies characteristic terms of the diffraction coefficient. It makes the diffraction coefficient applicable to dielectric wedges common in practical applications. In mobile communication scenarios, the horizontal distances are usually much greater than the vertical distances. Thus, the incidence angle is approximately normal. Parallel and perpendicular field polarizations are tested. The new heuristic diffraction coefficient shows clear accuracy improvement over existing heuristic coefficients when compared to the rigorous solution. Moreover, the proposed diffraction coefficient is simple to compute.

Papers [**P3**] improves the accuracy of an existing heuristic diffraction coefficient, i.e., Holm's, in the illumination region when the source illuminates one face of the wedge (i.e., building corner). This work improves Holm's diffraction coefficient in the illumination region by redefining reflection angles used

in the calculation of Fresnel reflection coefficient involved in the computation of the diffraction coefficient. The improved diffraction coefficient gives results that are very close to the Maliuzhinets (i.e., rigorous) diffraction coefficient. The improvement is valid for parallel and perpendicular field polarizations. The improved version of the diffraction coefficient has almost the same computational efficiency as the original implementation and is very close to the rigorous solution.

In paper [**P4**] diffuse scattering in urban environment is investigated through both the analysis of experimental results and the comparison between measurements with advanced 3D ray-tracing model, which takes diffuse scattering into account. The comparison is in performed terms of path loss, delay and direction spreads in a small cell. Diffuse scattering of the radio wave is especially relevant in the case of far buildings, which are very unlikely to produce significant reflection/diffraction effects. Far buildings are of major importance in the determination of channel dispersion and thus the wideband behavior of the urban mobile radio channel cannot be understood without taking diffuse scattering into account. The results show that diffuse scattering may play a key role in urban propagation, with a particular impact on the delay and angular spread of the signal at the receiver.

Papers [**P5**] and [**P6**] present wideband propagation models for radio wave propagation in the main and perpendicular streets, of an urban street grid for microcellular communications, respectively. The modeling approach of this work is ray-based. It considers possible coupling paths of different combinations of propagation mechanisms that couple the base station with the mobile station. The height of antennas is assumed to be below the rooftops of the surrounding buildings. The developed models are presented as explicit mathematical expressions. Analytical expressions of the spatial variant multi-ray channel transfer function are derived for every street type. The models provide characteristics of each ray in explicit expressions. The ray characteristics are given in terms of complex amplitude for both vertical and horizontal polarizations, path length, angle of arrival and departure. In order to check for rays that couple the BS to the MS, sets of angles in the horizontal plane are used to utilize set membership criteria to determine the coupling radio paths that join the BS with the MS. The presented models are easy to implement and fast to compute since only those rays that reach the receiver locations are considered.

In paper [**P7**], a new principle for path loss modeling is presented. The proposed technique is based on secondary source principle, which maps NLOS propagation problem to LOS propagation problem assuming that the dominant power arriving at the MS is from the secondary source. The model is intended for calculation of path loss of radio wave propagation in a perpendicular street. The model is given in a mathematical closed form, which takes into account information about the position of the BS and the MS in microcellular environment. The mathematical formulation of the model is based on the principle that the power leakage in the side street is regarded as the power of a secondary source for the propagation of radio waves in to the perpendicular street. The model fits quite well in the measurement results.

Paper [**P8**] presents characterization of the microcellular radio channel, where the BS is below the surrounding buildings, in terms of the influence of bandwidth on temporal propagation characteristics. The new frequency bands that will be allocated to enhanced-IMT2000 cellular networks might open the possibility to use higher bandwidths than the 5 MHz specified in 3GPP. The studied temporal characteristics are power delay profiles in terms of number of active fingers of CDMA Rake receiver and their power contribution to the total power. The power delay profiles with lower bandwidths (*i.e.*, 5, 10, and 20 MHz) are obtained by filtering down the processed measured impulse responses with bandwidth of 30 MHz. The paper presents characterization of the radio channel in terms of variation of the number of active fingers along traveling route for each bandwidth, number of active fingers that can capture at least 90% of the total power with probability of at least 90% and the influence of the bandwidth on the captured power of the first, i.e., strongest, finger. It has been shown that in a perpendicular street, doubling the bandwidth requires one more finger to capture the power of at least 0.5 dB less than the total power with about 90 % probability. Two fingers are active in all locations.

The contribution of the power of the first finger to the total power decreases with increasing the bandwidth.

Paper [**P9**] characterizes the radio channel in small cells, where the BS is above rooftops of buildings and the MS is traveling along a route in area close to the BS. The characterization of the radio channel takes place in path domain in order to obtain required information for DS-CDMA system design. The characterization results may help in optimizing Rake receiver design. The paper presents channel characterization in terms of the number of active fingers and their life distance, their PDF and CDF of relative power, contribution of powers of the fingers to the total received power, and the percentage of locations having certain number of fingers. The channel characterization is presented for 30 MHz and 5 MHz bandwidths. It is found that two fingers are active in all locations for 30 MHz bandwidth and more than 90 % for 5 MHz bandwidth. Half of the locations have seven and three active fingers for 30 MHz and 5 MHz bandwidths, respectively. The median of the second and third finger life distance, which is defined in [**P10**], is about 2 m for 5 MHz and 30 MHz bandwidths, respectively. The median power of the second finger is about 2 dB below the first finger power for both 5 MHz and 30 MHz bandwidths. The median power of the third finger with 5 MHz and 30 MHz bandwidth is about 4±0.5 dB below the first finger power, respectively. Ordering the fingers according to their power shows that the first (i.e., the strongest), second and third fingers have a major power contribution to the total power. Effect of spatial domain on the number of active fingers between two spaced antennas is also presented. Spatial domain has no effect on the statistical distribution of the number of fingers.

Paper [**P10**] characterizes the finger life distance of microcellular radio channels. It is defined in the paper as the distance along a street over which the finger is active, i.e., within a threshold of the peak. For a given mobile speed, the finger life distance is proportional to the finger lifetime, which is useful in specifying the search rate of the acquisition circuit in the Rake receiver. The results show that for a bandwidth of 30 MHz, the second finger is always active on the NLOS along a parallel street route when using a 10 dB threshold and when the height of the BS antenna is 3 m. The second finger of a system with 5 MHz bandwidth has a life distance less than 3.5 m and 12.5 m at the probability of 90% along routes in perpendicular and parallel streets, respectively. The maximum and mean of finger life distance decrease with increasing finger order.

6. Conclusion and future work

Contributions of this thesis can be categorized in three groups: a) development of diffraction coefficient, b) development of propagation model for urban street grid, c) characterization of radio channel for future mobile communications. It has been shown that the commonly used heuristic diffraction coefficient (i.e., Luebbers') and its extended version (i.e., Holm's) can lead to inaccurate results. This thesis proposes new heuristic diffraction coefficients and improves an existing one. The proposed solutions of diffraction processes for solid wedges are valid for normal incidence with respect to the edge axis of the wedge. The first proposed diffraction coefficient, (i.e., for hollow wedges), is based on absorbing wedge solution. The second proposed diffraction coefficient, (i.e., for solid wedges) is based on the PC-UTD. It has been shown that the second new heuristic diffraction coefficient is valid for the diffraction in the illumination and diffraction regions. The third contribution in diffraction modeling that presented in this thesis is improvement to an existing heuristic UTD diffraction coefficient (i.e., Holm's) for non-perfectly conducting wedges. The improvement enables more accurate prediction of diffracted field for any observation angle when the source illuminates only one face of the wedge and is valid for both parallel and perpendicular field polarizations. The proposed solutions have almost the same computational efficiency as the commonly used solutions.

Investigations of importance of diffuse scattering show that it may play a key role in urban propagation with particular impact on time delay and on angular spreads of the received signal at the receiver.

The second part of the thesis presents explicit expression models for radio wave propagation in the main and perpendicular streets of urban street grid for microcellular communications. The presented models are simple to implement and computationally fast. Each model of different propagation scenario, *i.e.,* streets, provides ray propagation information at both the BS and MS. The developed model determines the coupling radio paths based on set membership criteria. An approach based on secondary source principle for path loss modeling in perpendicular street is also presented. The mathematical formulation of the model is based on the principle that the power leakage into the side street is regarded as the power of a dominant secondary source of radio waves propagate into the side street.

The proposed explicit mathematical expression model is not only capable to provide macroscopic quantities like mean field values and rms delay spread, but also the full wideband channel information, *i.e.,* space dependent complex channel responses with a high time dispersion resolution. It can be applied in studying propagation problems in microcellular environment, e.g., diversity techniques, estimating MIMO capacity in city grid, evaluation of the influence of different antennas pattern and geometries on MIMO capacity, influence of bandwidth on temporal characteristics such number of effective fingers, orthogonality factors for W-CDMA downlink channel, etc.

The third part of the thesis deals with urban channel characterizations for extracting parameters that help in successful design of future mobile communication systems. The developed models can be used to characterize radio channels in street grids. Wideband measurement results at 2 GHz in microcell scenario have been analyzed for radio channel characterization for future enhanced-IMT2000 system having bandwidth wider than 5 MHz. It has been shown that in a perpendicular street, doubling the bandwidth requires one more finger to meet the quality of service criterion. Finger characteristics for small cells scenarios have also been investigated. Channel characterization in path domain is presented in terms of the number of active fingers, their relative power PDF and CDF, contribution of the finger powers to the total received power, and the percentage of locations having certain number of fingers. Spatial domain was not found to have an effect on the statistical distribution of the number of active fingers. Finger life distance has also been investigated for both small cell and microcell scenarios. The channel orthogonality factor is very important for W-CDMA downlink capacity analysis. It has been shown that the currently used values of orthogonality factor, for the W-CDMA system of 5 MHz bandwidth, are unlikely to be reliable for higher bandwidth that might be used for enhanced-IMT2000 system as they may overestimate the capacity of the system. Direction and delay spread have been characterized for microcellular scenario at two different base station antenna heights. It is observed that direction spread is affected by different heights of antennas in the LOS scenario, while no significant change in the CDF with antenna height is seen for NLOS perpendicular and parallel streets. The influence of the antenna height on the delay spread is higher for LOS scenarios than the NLOS streets. The correlation between the direction spread and delay spread in microcellular scenarios is high for the LOS cases with two antenna heights. Low correlation is noticed for NLOS streets at both heights of the BS antenna. A measure that expresses a grade of (dis-) similarity between different multipath components in different domains has been introduced. It shows that in LOS scenario considerable amount of components arrive the mobile station from opposite directions, i.e., two main clusters in angular domain, for the studied geometry. There are many components arrive at the MS as back scattering.

As future work, the explicit expression model will be extended to include parallel street model and in addition, diffuse scattering process will be included. Then, analyzed multidimensional channel measurement results are utilized to find distributions of random components that are superimposed on deterministic components to add them to the explicit model to make it more reliable for applications such as spatio-temporal channel model for an urban street grid. The other future work is related to the characterization of the channels. This will focus on finding statistical distributions for Rake finger characteristics and orthogonality factor for different environments. Extension of the work to measure

(dis-) similarity between multipath components is performed as a step toward multipath clustering analysis in order to develop an algorithm that can extract and define clustering properties from huge amount of measurement data since most of the current available technique is visual inspection. Further investigation that is needed for the secondary source modeling approach for both perpendicular and parallel streets is also part of the future work.

In summary, the significances of this work in this area of science are: 1) development of more accurate and computationally efficient diffraction coefficient that can be used in propagation prediction tools for mobile communications systems, 2) development of computationally efficient wideband propagation models, which researchers can easily use for studying propagation problems in microcellualr urban street grids, 3) providing channel parameters that help system designers of future mobile communications systems.

REFERENCES

[1] N. Chandarn and M.C. Valenti, "Three generations of cellular wireless systems," *IEEE Potentials*, vol. 20, no. 1, pp. 32–35, Feb.-March 2001.

[2] T. Ojampera, R. Prasad, "An overview of air interface multiple access for IMT-2000/UMTS," *IEEE Commun. Mag*. vol. 36, no. 9, pp. 82–95, Sept. 1998.

[3] 3GPP recommendation #3GTS25.212 v3.3.0 (2000-06).

[4] Source: Output of the 6th ITU-R WP8F, Oct. 2001, 8F/TEMP/205 Rev. 1.

[5] J. Takada, Fu Jiye, Z. Houtao, and T. Kobayashi "Spatio-temporal channel characterization in a suburban non line-of-sight microcellular environment," *IEEE J. Select. Areas Commun*. vol. 20, no. 3, pp. 532–538, Apr. 2002.

[6] D. Har and H.L. Bertoni, "Effect of anisotropic propagation modeling on microcellular system design," *IEEE Trans. Veh. Technol.,* vol. 49, pp. 1303–1313, July 2000.

[7] J.C. Bultitude and G.K. Bedal, "Propagation characteristics on microcellular urban mobile radio channels at 910 MHz," *IEEE J. Select. Areas Commun*., vol. 7, no. 1, pp. 31–39, Jan. 1989.

[8] A. Kuchar, J.-P. Rossi, and E. Bonek, "Directional macro-cell channel characterization from urban measurements," *IEEE Trans. Antennas and Propagat.,* vol. 48, no. 2, pp.137–146, Feb. 2000.

[9] Y.L.C. De Jong and M.H.A.J. Herben, "High-resolution angle-of-arrival measurement of the mobile radio channel," *IEEE Trans. Antennas and Propagat.,* vol. 47, pp.1677–1687, Nov. 1999.

[10] B. H. Fleury and P. E. Leuthold, "Radiowave propagation in mobile communications: an overview of European research," *IEEE Commun. Mag*. vol. 50, no. 3, pp. 662–673, March 2002.

[11] M.F. Iskander and Y. Zhengqing "Propagation prediction models for wireless communication systems," *IEEE Trans. Microwave Theory and Techniques.,* vol. 43, 1058–1066, Nov. 1994.

[12] H.L. Bertoni, W. Honcharenko, L.R. Maciel and H.H. Xia, "UHF propagation for wireless personal communications," *IEEE Proc.*, vol. 82, 1333–1359, Sep. 1994.

[13] U. Dersch, and E. Zollinger, "Propagation mechanisms in microcell and indoor environment," *IEEE Trans. Antennas and Propagat.,* vol. 43, 1058–1066, Nov. 1994.

[14] C. Kloch, G. Liang, J. Bach Andersen, G.F. Pedersen, and H.L. Bertoni, "Comparison of measured and predicted time dispersion and direction of arrival for multipath in a small cell environment," *IEEE Trans. Antennas and Propagat.,* vol. 49, no. 9 1254–1263, Sep. 2001.

[15] S.Y. Seidel, T.S. Rappaport, S. Jain, M.L. Lord, R. Singh, "Path loss, scattering and multipath delay statistics in four European cities for digital cellular and microcellular radiotelephone," *IEEE Trans. Veh. Technol*., vol. 40, no. 4, pp. 721–730, Nov. 1991.

[16] J.H. Tarng and K.M. Ju "A novel 3-D scattering model of 1.8-GHz radio propagation in microcellular urban environment," *IEEE Trans. on Electromagnetic Compatibility*, vol. 41, no. 2, pp. 100–106, May 999.

[17] S.Y. Tan and H.S. Tan. "A microcellular communications propagation model based on the uniform theory of diffraction and multiple image theory," *IEEE Trans. Antennas and Propagat.,* vol. 44, no. 10, pp. 1317–1326, Oct. 1996.

[18] J. Bach Andersen, T.S. Rappaport, and S. Yoshida, "Propagation measurements and models for wireless communications channels," *IEEE Antennas and Propagation Magazine,* vol. 33, no. 1, pp. 42–49, Jan. 1995.

[19] R.S. Thoma, etal "Identification of time-variant directional mobile radio channels**,**" *IEEE Trans. on Instrument. and Measurem.,* vol. 49, no. 2, pp. 357–364, Apr. 2000.

[20] J. Laurila, K. Kalliola, M. Toeltsch, K. Huhgl, P. Vainikainen, and E. Bonek, "Wide-band 3-D characterization of mobile radio channels in urban environment," *IEEE Trans. on Antennas and Propagat.* vol. 50, no. 2, pp. 233–243, Feb. 2002.

[21] K. Kalliola, H. Laitinen, P. Vainikainen, and L.I. Vaskelainen; "Real-time 3-D spatial-temporal dual-polarized measurement of wideband radio channel at mobile station," *IEEE Trans. on Instrument. and Measurem.* vol. 49, no. 2, pp. 439–448, Apr. 2000.

[22] A.J. Paulraj, C.B. Papadias, "Space-time processing for wireless communications, improving capacity, coverage, and quality in wireless networks by exploiting the spatial dimension," *IEEE Signal Processing Magazine,* vol. 14, no. 5, pp. 49–83, Nov. 1997.

[23] R. Kohno "Spatial and temporal communication theory using adaptive antenna array" *IEEE Personal Communications,* vol. 5, no. 1, pp. 28–35, Feb. 1998.

[24] C.B. Dietrich, Jr., W.L. Stutzman, K. Byung-Ki, and K. Dietze, "Smart antennas in wireless communications: base station diversity and handset beamforming," *IEEE Antennas and Propagation Magazine,* vol. 42, no. 5, pp. 142–151, October 2000.

[25] G.J. Foschini and M.J. Gans, "On limits of wireless communication in fading environment when using multiple antennas," *Wireless Personal Communications*, vol. 6, no. 3, pp. 311–335, March 1998.

[26] J. Bach Andersen, "Antenna arrays in mobile communications: gain, diversity, and channel capacity," *IEEE Antennas and Propagation Magazine,* vol. 42, no. 2, pp. 12–16, Apr. 2000.

[27] J. Bach Andersen, "Array gain and capacity for known random channels with multiple element arrays at both ends," *IEEE J. Select. Areas Commun*., vol. 18, no. 11, pp. 2172–2178, Nov. 2000.

[28] M.C. Lawton and J.P. McGeehan, "The application of a deterministic ray launching algorithm for the prediction of radio channel characteristics in small-cell environments," *IEEE Trans. Veh. Technol*., vol. 43, pp. 955–969, Nov. 1994.

[29] G.E. Athanasiadou, A.R. Nix, and J.P. McGeehan, "A microcellular ray tracing model and evaluation of its narrow-band and wide-band predictions," *IEEE J. Select. Areas Commun*., vol. 18, no. 3, pp. 322–355, Mar. 2000.

[30] G.E. Athanasiadou and A.R. Nix, "A novel 3-D indoor ray-tracing propagation model: the path generator and evaluation of narrow-band and wide-band predictions," *IEEE Trans. Veh. Technol*., vol. 49, pp. 1152–1168, July 2000.

[31] G. Liang and H. Bertoni, "A new approach to 3-D ray tracing for propagation prediction in cities," *IEEE Trans. Antennas Propagat*., vol. 46, no. 6, pp. 853–863, June 1998.

[32] J.P. Rossi, J.C. Bic, A.J. Levy, Y. Gabillet, and M. Rosan, "A ray launching method for radio mobile propagation in urban area," *IEEE APS symposium* Digest, pp. 1540–1543, 1991.

[33] S.Y. Tan and H.S. Tan, "A microcellular communications propagation model based on the uniform theory of diffraction and multiple image theory," *IEEE Trans. Antennas and Propagat.,* vol. 44, pp.1317–1326, Oct. 1996.

[34] K. Rizk , J.-F. Wagen, and F. Gardiol, "Two-dimensional ray tracing modeling for propagation in microcellular environments," *IEEE Trans. Veh. Technol.,* vol. 46, pp. 508–518, Feb. 1997.

[35] A.G. Kanatas, I.D. Kounouris, G.B. Kostaras, and P. Constantinou, "A UTD propagation model in urban microcellular environments," *IEEE Trans. Veh. Technol.,* vol. 46, pp. 185–193, Jan. 1997.

[36] V. Erceg, S.J. Fortune, J. Ling, A.J. Rustako, and R. A. Valenzuela, "Comparisons of a computer-based propagation prediction tool with experimental data collected in urban microcellular environments," *IEEE J. Select. Areas Commun*., vol. 15, pp. 677–684, May 1997.

[37] H.R. Anderson, "A ray tracing propagation model for digital broadcasting systems in urban areas," *IEEE Trans. Broadcasting,* vol. 39, pp. 309–317, Sep. 1993.

[38] G.V. Tsoulos and G. Athanasiadou, "On the application of adaptive antennas to microcellular environments: radio channel characteristics and system performance," *IEEE Trans. Veh. Technol.,* vol. 51, pp. 1–16, Jan. 2002.

[39] A. Taflove, *Computational electrodynamics: the finite-difference time-domain method.* Norwood, MA: Artech House, 1995.

[40] T.S. Rappaport, *Wireless communications, principles and practice*, Upper Saddle River, NJ: Prentice Hall, 1996.

[41] J.D. Gibson*, The mobile communications Handbook*, CRC press, Inc., 1996.

[42] J. Kivinen, "Development of wideband radio channel measurement and modeling techniques for future radio systems," *Report S244, Doctoral thesis*, March 2001, Helsinki University of Technology.

[43] W.L. Stutzman, *Polarization in electromagnetic systems*, Artech House,Boston,1993.

[44] D.A. McNamara, C.W.I. Pistorius, and J.A.G. Malherbe, *Introduction to the uniform geometrical theory of diffraction*, Artech House, Boston, London, 1996.

[45] R.G. Kouyoumjian and P.H. Pathak, "A uniform geometrical theory of diffraction for and edge in a perfectly conducting surface," *IEEE Proc.,* vol. 62, pp. 1448–1461, Nov. 1974.

[46] L.B. Felsen and N. Marcuvitz, *Radiation and scattering of wave*s. Englewood Cliffs, NJ: Prentice-Hall, 1973.

[47] R.G. Rojas, "Electromagnetic diffraction of an obliquely incident plane wave field by a wedge with impedance faces," *IEEE Trans. Antennas Propagat*., vol. 36, pp. 956–970, July 1988.

[48] R. Tiberio, G. Pelosi, G. Manara, and P.H. Pathak, "High-frequency scattering from a wedge with impedance faces illuminated by a line source – Part I: Diffraction," *IEEE Trans. Antennas Propagat.*, vol. 37, pp. 212–218, Feb. 1989.

[49] G. Pelosi, G. Manara, and P. Nepa, "Diffraction by a wedge with variable-impedance faces," *IEEE Trans. Antennas Propagat.*, vol. 44, pp. 1334–1340, Oct. 1996.

[50] M.F. Otero and R.G. Rojas, "Two-dimensional Green's function for a wedge with impedance faces," *IEEE Trans. Antennas Propagat.*, vol. 45, pp. 1799–1809, Dec. 1997.

[51] G.D. Maliuzhinets, "Excitation, reflection and emission of surface waves from a wedge with given face impedances," *Sov. Phys. Dokl.,* vol. 3, no. 4, pp. 752–755, 1958.

[52] R.J. Luebbers, "Finite conductivity uniform UTD versus knife diffraction prediction of propagation path loss," *IEEE Trans. Antennas Propagat*., vol. 32, pp. 70–76, Jan. 1984.

[53] R.J. Luebbers, "A heuristic UTD slope diffraction coefficient for rough lossy wedges," *IEEE Trans. Antennas Propagat*., vol. 37, pp. 206–211, Feb. 1989.
[54] K.A. Remely, H.R. Anderson, and A. Weisshar, "Improving the accuracy of ray tracing techniques for indoor propagation modeling," *IEEE Trans. Veh. Technol*., vol. 49, pp. 2350–2357, Nov. 2000.
[55] K.A. Remely, H.R. Anderson, and A. Weisshar, "Improved diffraction coefficients for lossy dielectric wedges," *Electronics Letters*, vol. 35, no. 21, pp.1826–1827, Oct. 1999.
[56] P.D. Holm, "A new heuristic UTD diffraction coefficient for nonperfectly conducting wedges," *IEEE Trans. Antennas Propagat*., vol. 48, pp. 1211-1219, Aug. 2000.
[57] R. Tiberio, A. Toccafondi, and F. Mioc, "High-frequency diffraction at the edge of a dielectric screen," in *Proc. of International Microwave and Optoelectronics Conference,* SBMO/IEEE MTT-S, APS and LEOS-IMOC'99, pp. 490–492, vol. 2, 1999.
[58] O. Landdron, M.J. Feuerstein, and T.S. Rappaport, "A comparison of theoretical and empirical reflection coefficients for typical exterior wall surfaces in mobile radio environment," *IEEE Trans. Antennas Propagat*., vol. 44, pp. 341-351, Mar. 1996.
[59] V. Degli-Esposti "A diffuse scattering model for urban propagation prediction," *IEEE Trans. Antennas Propagat*., vol. 49, pp. 1111–1113, July, 2001.
[60] V. Degli-Esposti and H.L. Bertoni, "Evaluation of the role of diffuse scattering in urban microcellular propagation," *Proc. IEEE Vehic. Technol. Conf.* (VTC'99-fall), Amsterdam, The Netherland, Sept. 19–22, 1999.
[61] M.D. Yacoub, *Foundations of mobile radio engineering*, CRC press Inc. 1993.
[62] H.L. Bertoni, *Radio propagation for modern wireless systems*, Prentice Hall, 2000.
[63] J. Rustaku, N. Amitay, G. J. Owens, and R. R. Roman, "Radio propagation at microwave frequencies for line-of-sight microcellular mobile and personal communications," *IEEE Trans. Vehic. Tech.*, vol. 40, pp. 203–210, Feb. 1991.
[64] H.H. Xia, H.L. Bertoni, L.R. Maciel, A. Lindsay-Stewart, and R. Rowe, "Radio propagation characteristics for line-of-sight microcellular and personal communications," *IEEE Trans. Antennas Propagat.*, vol. 41, pp. 1439–1447, Oct. 1993.
[65] Y. Oda, K. Tsunekawa, and M. Hata, "Advanced LOS path-loss model in microcellular mobile communications," *IEEE Trans. Veh. Technol.*, vol. 49, pp. 2121–2125, Nov. 2000.
[66] W.C.Y. Lee and D.J.Y. Lee, "Microcell prediction in dense urban area," *IEEE Trans. Veh. Technol.*, vol. 47, pp. 246–253, Feb. 1998.
[67] N.C. Goncalves and L.M. Correia, "A propagation model for urban microcellular systems at the UHF band," *IEEE Trans. Veh. Technol.*, vol. 49, pp. 1294–1302, July 2000.
[68] J. Berg, "A recursive method for street microcell path loss calculations," in *Proc. PIMRC'95*, pp. 140–143.
[69] L.M. Correia, *Wireless flexible personalized communications*, John Wiley and Sons, 2001, 462 p.
[70] R.A. Mazar, A. Bronshtein, and I.-T. Lu, "Theoretical analysis of UHF propagation in a city street modeled as a random multislit waveguide," *IEEE Trans. Antennas and Propagat.,* vol. 46, 864–871, Jun. 1998.
[71] Y. Tan, and H.S. Tan, "UTD propagation model in an urban street scene for microcellular," *IEEE Electromag. Compat.,* vol. 35, pp. 423–428, Nov. 1993.
[72] D. Har, H.H. Xia, and H.L. Bertoni, "Path-loss prediction model for microcells" *IEEE Trans. Veh. Technol.*, vol. 48, pp. 1453–1462, Sep. 1999.
[73] W.C.Y. Lee and D.J.Y. Lee, "Pathloss predictions from microcell to macrocell," in *Proc. IEEE Vehicl. Technolo.* VTC2000-Spring, vol. 3, pp. 1988–1992, May, 2000, Tokyo, Japan.
[74] H. Zhu, J. Fu, J. Takada, K. Araki, and H. Masui "A spatio-temporal channel measurement and ray-tracing validation in suburban microcell environments," in *Proc. IEEE AP-S International Conf*., pp. 1138–1141, 2000.

[75] S. Ichitsubo, T. Furuno, T. Taga, and R. Kawasaki, "Multipath propagation model for line-of-sight street microcells in urban area" *IEEE Trans. Veh. Technol.*, vol. 49, pp. 422–427, March 2000.

[76] G. Lampard and V.D. Dinh, "The effect of terrain on radio propagation in urban microcells," *IEEE Trans. Veh. Technol.,* vol. 42, no. 3, pp. 314–317, 1993.

[77] F. Ikegami, S. Yoshida, T. Takeuchi, and M. Umehira, "Propagation factors controlling mean field strength on urban street," *IEEE Trans.Antennas Propagat.,* vol. AP-32, no. 8, pp. 822–829, 1984.

[78] J. Walfish and H. Bertoni, "A theoretical model of UHF propagation in urban environments," *IEEE Trans. Antennas Propagat.,* vol. 36, no. 12, pp. 1788–1796, 1988.

[79] A.J. Rustako, N. Amitay, G.J. Owens, and R.S. Roman, "Radio propagation at microwave frequencies of LOS microcellular mobile and personal communication," *IEEE Trans. Veh. Technol.,* vol. 40, pp. 203–210, Feb. 1991.

[80] J.H. Whitteker, "Measurements of path loss at 910 MHz for proposed microcell urban mobile systems," *IEEE Trans. Veh. Technol.,* vol. 37, pp. 125–129, Aug. 1988.

[81] P. Harley, "Short distance attenuation measurement at 900 MHz and 1.8 GHz using low antenna height for microcells," *IEEE J. Select. Areas Commun.,* vol. 7, pp. 5–11, Jan. 1989.

[82] K.R. Schaubach, and N.J. Davis "Microcellular radio-channel propagation prediction" *IEEE Antennas and Propagat. Magazine*, vol. 36, no. 4, pp. 25-34, Aug. 1994.

[83] T. Taga, T. Furuno, K. Suwa, **"**Channel modeling for 2-GHz-band urban line-of-sight street microcells," *IEEE Trans. Veh. Technol.,* vol. 48, pp. 262–272, Jan. 1999.

[84] A.J. Goldsmith, and L.J. Greenstein, **"**A measurement-based model for predicting coverage areas of urban microcells" *IEEE J. Select. Areas Commun*., vol. 11, no. 7, pp. 1013–1023, Sep. 1993.

[85] W.M. O'Brien, E.M. Kenny, and P.J. Cullen, "An efficient implementation of a three-dimensional microcell propagation tool for indoor and outdoor urban environments" *IEEE Trans. Veh. Technol.,* vol. 47, no. 2, pp. 622–630, Mar. 2000.

[86] J.-I. Takada, W. Hachtani, J.Y. Fu, and H. Zhu, "Site-specific stochastic spatio-temporal channel model for sub-urban slightly non-line-of-sight microcellular environment," *COST 273 WORKSHOP, Opportunities of the Multidimensional Propagation Channel*, Espoo, Finland, May 2002.

[87] H.M. El-Sallabi, "Characterization of separation distance of multipath components at mobile station in microcellular environment," *manuscript prepared for journal submission*.

[88] H.M. El-Sallabi "Modeling of diffraction multipath components and channel characterization for radio wave propagation in a main city street," *manuscript prepared for journal submission*.

[89] R.J.C. Bultitude "A comparison of multipath dispersion related microcellular mobile radio channel characteristics at 1.9 GHz and 5.8 GHz," in *Proc. Symposium on Antenna Technology and Applied Electromagnetics* (ANTEM 2002), Montreal, July 31-Aug. 2, 2002. pp. 632–626.

[90] T.C.W. Schenk, and R.J.C. Bultitude, etal, "Analysis of propagation loss in urban microcells at 1.9 GH and 5.8 GHz," in *Proc. URSI commission F Open Symposium on Radio Wave propagation and Remote Sense*, Germany, Feb. 12-15, 2002.

[91] H. Xu, D. Chizhik, H. Huang, and R. Valenzuela, "A wave-based wideband MIMO channel modeling technique**,**" in *Proc. of the 13th IEEE International Symposium on Personal, Indoor and Mobile Radio Communication* (PIMRC2002), vol. 4, pp. 1626–1630, London UK, Sept. 15-18, 2002.

[92] F. Molisch, "A channel model for MIMO systems in macro- and microcellular environments," in *Proc. IEEE Commun. Conf.* (ICC2002). vol. 1, pp. 277–282, 2002. NYC, USA.

[93] A. F. Molisch, "A generic model for MIMO wireless propagation channels," *Proc. IEEE Vehicl. Technol. Conf*. VTC2000-Spring, vol. 2, pp. 655–659, May, 2002.

[94] H.M. El-Sallabi and Jouni Tervonen, "Polarization dependence of multipath propagation characteristics in line of sight microcellular channels," in *Proc.* of *the 12th International Conference on Wireless Communications* (Wireless2000) Alberta, Calgary, Canada, July 10-12, 2000.

[95] H.M. El-Sallabi, "Polarization consideration in characterizing radio wave propagation in urban microcellular channels," in *Proc. of the 11th IEEE International Symposium on Personal, Indoor and Mobile Radio Communication* (PIMRC2000), pp. 411–415, London UK, September 18-21, 2000.

[96] H.M. El-Sallabi, and Pertti Vainikainen, "Investigations of controlling propagation characteristics using antenna array in mobile microcellular environment," in *Proc. of joint ICAP and JINA, AP2000 Millennium Conference on Antennas & Propagation,* Davos, Switzerland, April 9-14, 2000.

[97] H.M. El-Sallabi and Jouni Tervonen, "A model-based characterization of microcellular space and frequency diversity," in *Proc. of the 2000 European Conference on Wireless Technology* (ECWT2000), on 5-6 Oct. 2000 in Paris, France.

[98] H. Holma and A. Toskala (Editors), *WCDMA for UMTS - radio access for third generation mobile communications*, John Wiley and Sons, Second Edition, 2000.

[99] J. Laiho, A. Wacker, T. Novosad (Editors), *Radio Network Planning and Optimization for UMTS*, John Wiley & Sons, 2002.

[100] K.I. Pedersen and P.E. Mogensen, "The downlink orthogonality factors influence on WCDMA system performance," in *Proc. of the* 56th *IEEE Veh. Technolog. conference* VTC2002-fall, vol. 4, pp. 2061–2065, 2002.

[101] V. DaSilva, E.S. Sousa, "Performance of orthogonal CDMA codes for quasi-synchronous communication systems," *IEEE Proc ICUPC*, pp. 995–999, 1993.

[102] M. Humukumbure, M. Beach, B. Allen, "Downlink orthogonality factor in UTRA FDD systems," *IEE Electronics Letters*, vol. 38, no. 4, pp. 196-197, February 2002.

[103] N.B. Mehta, L.J. Greenstein, T.M. Willis, Z. Kostic, "Analysis and results for the orthogonality factor in WCDMA downlinks," *IEEE Proc. of Vehicular Technology Conference*, pp. 100–104, May 2002.

[104] C. Passerini and G. Falciasecca, "Correlation between delay-spread and orthogonality in urban environments," *IEE Electronics Letters*, vol. 37, no. 6, pp. 384–385, March 2001.

[105] P. Eggers "Angular propagation descriptions relevant for base station adaptive antenna operations," *Wireless Personal Commun., Special Issue on SDMA*, vol. 11, pp. 3–29, 1999.

[106] G. Durgin and T. Rappaport, "Theory of multipath shape factors for small-scale fading wireless channels," *IEEE Trans. Antennas Propagat.*, vol. 48, no. 5, pp. 682–693, May 2000.

[107] B. H. Fleury, "First- and second-order characterization of direction dispersion and space selectivity in the radio channel," *IEEE Trans. on Inform. Theory*, vol. 46, no.6, pp. 2027–2044, Sep. 2000.

[108] C. Cheon, G. Liang, H.L. Bertoni, "Simulating radio channel statistics for different building environments,**"** *IEEE J. on Select. Areas in Commun.*, vol. 19, no. 11 , pp. 2191–2200, Nov. 2001.

[109] M. Steinbauer, etal "*How to quantify multipath separation,*" *IEICE Transactions on Electronics, Special Issue on Signals, Systems and Electronics Technology*, vol. E85-C, No. 3, pp. 552–557, Mar. 2002.

[110] D.E. Wilson and T.R. Martinez, "Improved heterogeneous distance functions," *Journal of Artificial Intelligence Research*, vol. 6:1, pp. 1–34, 1997.

[111] W. Zhang, J. Lähteenmäki, P. Vainikainen, and H.M. El-Sallabi, "Fast two-dimensional diffraction modeling for mobile radio propagation prediction in urban micro-cellular environments" in *Proc. 28th European Microwave Conf.* Amsterdam, The Netherland, pp. 362–367, Oct. 1998.

[112] N.G. Tarhuni and T.O. Korhonen “Influence of environment on capacity of LOS city street MIMO channel,” *URSI/IEEE XXVII Convention on Radio Science*, Oct. 2002, pp. 126–128, Finland.

HELSINKI UNIVERSITY OF TECHNOLOGY RADIO LABORATORY REPORTS

S 247 Juntunen, J.
Selected developments in computational electromagnetics for radio engineering, May 2001

S 248 Tretyakov, S.
Waveguide and Antenna Theory, July 2001

S 249 Kalliola, K., Sulonen, K., Laitinen, T., Kivekäs, O., Krogerus, J., Vainikainen, P.
Angular power distribution and mean effective gain of mobile antenna in different propagation environments, September 2001

S 250 Icheln, C.
Methods for measuring RF radiation properties of small antennas, November 2001

S 251 Kalliola, K.
Experimental analysis of multidimensional radio channels, February 2002

S 252 Ollikainen, J. , Vainikainen, P.
Design and bandwidth optimization of dual-resonant patch antennas, March 2002

S 253 Vainikainen, P., Lindberg, S. (editors)
HUT Radio Laboratory research and education 2001, April 2002

S 254 Dudorov, S.
Rectangular dielectric waveguide and its optimal transition to a metal waveguide, June 2002

S 255 Laiho, J.
Radio network planning and optimisation for WCDMA, July 2002

S 256 Zhao, X.
Multipath propagation characterization for terrestrial mobile and fixed microwave communications, October 2002

S 257 Tretyakov, S., Säily, J.
URSI/IEEE XXVII convention on radio science, October 2002

S 258 Säily, J., Räisänen, A.
Studies on specular and non-specular reflectivities of radar absorbing materials (ram) at submillimetre wavelengths, February 2003

S 259 Räisänen, A., Lindberg, S. (editors)
HUT Radio Laboratory research and education 2002, March 2003

S 260 Tretyakov, S., Maslovski, S.
International student seminar on microwave applications of novel physical phenomena, May 2003

ISBN 951-22-6627-X
ISSN 1456-3835